Rivista Italiana di Paleontologia e Stratigrafia	volume 108	numero 3	tavole 4	pagine 457-478	Novembre 2002

INTEGRATED HIGH-RESOLUTION STRATIGRAPHY OF THE LOWER OLIGOCENE TUSA TUFFITE FORMATION IN THE CALABRO-LUCANO AREA AND SICILY (SOUTHERN ITALY)

LUCA BARUFFINI, FABIO LOTTAROLI & STEFANO TORRICELLI

Received December 12, 2001; accepted May 3, 2002

Key-words: Biostratigraphy, Dinoflagellate cysts, Calcareous nannofossils, Turbidites, Volcaniclastic layers, Lower Oligocene, Southern Apennines, Italy.

Riassunto. Le argille intercalate alle torbiditi vulcanoclastiche ascritte alle Tufiti di Tusa, affioranti lungo la sezione stratigrafica di Canale Candela (confine Calabro-Lucano, Italia meridionale), hanno fornito associazioni a palinomorfi e nannoplancton calcareo ricche, diversificate e in buono stato di conservazione. Esse consentono di applicare le biozonazioni a dinoflagellate e nannofossili elaborate nell'ultimo decennio in successioni pelagiche dotate di ottimo controllo bio- e magnetostratigrafico presenti nell'Appennino centrale e settentrionale. L'aggancio alla scala cronostratigrafica standard così ottenuto, consente di attribuire con inedita precisione le Tufiti di Tusa della sezione di Canale Candela alla parte bassa dell'Oligocene inferiore.

I campioni delle Tufiti di Tusa prelevati nell'area tipo (Monti Nebrodi, Sicilia) hanno evidenziato associazioni a palinomorfi e nannofossili meno ricche e in peggiore stato di conservazione che, sebbene non consentano di elaborare una biostratigrafia integrata di dettaglio come nel caso della sezione di Canale Candela, attestano l'equivalenza di età tra queste torbiditi vulcanoclastiche e quelle presenti nell'area Calabro-Lucana.

L'attribuzione di entrambi gli affioramenti di Tufiti di Tusa all'Oligocene inferiore, unitamente alle somiglianze di facies, consentono di stabilire analogie con altre successioni vulcanoclastiche di età rupeliana del sistema Alpi/Appennino, in particolare con la Formazione della Val d'Aveto appartenente alle Unità Subliguri dell'Appennino settentrionale, con la Formazione di Ranzano appartenente alla successione Epiligure dell'Appennino settentrionale e con le Arenarie di Taveyanne delle Alpi occidentali. Ciò evidenzia l'esistenza di un unico evento di sollevamento e smantellamento di un arco vulcanico all'interno del sistema orogenico Alpi/Appennino durante l'Oligocene inferiore.

Abstract. Shale samples from the volcaniclastic turbidites ascribed to the Tusa Tuffite Formation (Tufiti di Tusa Auct.) cropping out at the Canale Candela section (Calabro-Lucano boundary, southern Italy) have yielded rich, diverse and well-preserved palynomorph and calcareous nannofossil assemblages. They allow the consistent recognition of both dinoflagellate cyst and calcareous nannofossil zones previously defined in bio- and magnetostratigraphically well calibrated pelagic sequences of the central and northern Apennines. Thus they give the Canale Candela section a first order correlation to the standard chronostratigraphic scale with high precision. On this basis, an earliest Oligocene age is assigned to this succession.

Poorly preserved sparse palynological and calcareous nannofossil assemblages have been recovered from the Tusa Tuffite at the type-locality (Nebrodi Mountains, NE Sicily). Hence, no biozonation is proposed for the Tusa section. The overall composition of the Tusa assemblages, however, unequivocally supports the correlation with the Canale Candela volcaniclastic turbidites.

The detailed age assessment of the Tusa Tuffite outcrops investigated, as well as facies similarities, give a broad regional correlation with other Rupelian volcaniclastic successions of the Alps/Apennines system, namely the Aveto Formation belonging to the Subligurian Domain of the northern Apennines, the Ranzano Formation belonging to the Epiligurian succession of the northern Apennines and the Taveyanne Sandstones of the western Alps. In this framework, we suggest that a single regional event of rise and erosion of a volcanic arc occurred in the Alps/Apennines orogenic system during the Early Oligocene.

Introduction

The Tusa Tuffite succession (Tufiti di Tusa Auct.) was originally described from north-eastern Sicily by Ogniben (1960) within the 'Sicilide Complex', as a distinctive facies characterizing the upper portion of the Polizzi Formation. Since its definition, the age of the Tusa Tuffite Formation, as well as the age of many other turbidites exposed in the Apennines, has been a much debated question. Although the authors have generally been in agreement in correlating the Sicilian Tusa Tuffite to similar volcaniclastic turbidites in the Calabro-Lucano area, the Late Eocene-Early Oligocene age stated for these deposits in both localities (Ogniben 1960, 1969) was not unanimously accepted.

Wezel (1973) and Guerrera & Wezel (1974) in Sicily, and Lentini (1979) at the Calabro-Lucano boundary, suggested for the Tusa Tuffite Formation a possible latest Oligocene-Aquitanian age based on scarce foraminiferal records. An Aquitanian-Burdigalian age

ENI S.p.A., Agip Division, P.O.Box 12069, 20100 Milano, Italy; e-mail: stefano.torricelli@agip.it

was assigned by Zuppetta et al. (1984) to sediments sampled at the section investigated in the present study (Canale Candela, southern Apennines) on the basis of only three samples deemed to be as age diagnostic for planktonic foraminifers.

In a paper focused on the Sicilide Units of the Sicilian Maghrebids, De Capoa et al. (2000) confirmed the scarcity and poor preservation of foraminiferal assemblages recovered from the Tusa Tuffite in the type-area and presented the results of a calcareous nannofossil study of this unit. Relying on the sporadic occurrences of *Discoaster druggii, Geminilithella rotula, Helicosphaera carteri, Sphenolithus belemnos* and *Triquetrorabdulus milowii*, they determined an age not older than early Burdigalian. Unfortunately, as well as in the other papers mentioned above, neither quantitative data nor fossil illustrations are shown. De Capoa et al. (2000) argued that, following previous papers which led to younger assessment of formations formerly considered Cretaceous or Paleogene in age, 'reworking of coccoliths and foraminifers in turbiditic successions must be retained as systematic and criteria useful to distinguish reworked and unreworked taxa do not exist'. At the same time those authors stated that 'all the collected samples are characterized by the prevalence of reworked taxa (up to 90% and more)', and 'Last Appearance Datums as well as state of preservation and quantitative analyses are meaningless in turbiditic sediments'. In our opinion these statements are questionable, since quantitative analytical methods have been extensively and succesfully applied to nannofossil and palynomorph assemblages recovered from Paleogene and Neogene turbidites both in the northern Apennines (Fornaciari et al. 1996; Fornaciari & Rio 1996; Catanzariti et al. 1997) and in the southern Apennines (Maiorano 1998; Torricelli 2000; Torricelli & Biffi 2001).

Implications arising from the chronostratigraphic attribution of the Tusa Tuffite Formation are a key point for the paleogeodynamic model of the Alps/Apennines orogenic system. The presence of volcaniclastic beds in the upper part of the succession, in an actualistic view, is related to the rise and erosion of a volcanic arc in a subduction zone (Critelli et al. 1990). Hence, the correlation of the Tusa Tuffite with other Rupelian volcaniclastic beds distributed in the northern Apennines (Cibin et al. 1998, Elter et al. 1999) and in the western Alps (Latelin & Muller 1987) would indicate a unique volcanic arc event spanning a relatively short time interval in the Early Oligocene. By contrast, a Miocene age of the Tusa Tuffite Formation would indicate a significant diachronism of the orogenic volcanism in different sectors of the Alps/Apennines system.

In this controversial framework, we approached the study of the Tusa Tuffite Formation by integrating palynomorph and calcareous nannofossil biostratigraphies, physical stratigraphy and sedimentology of turbidites. A complete documentation of the analytical data is presented, including quantitative occurrence-charts and photographic illustrations of fossils, and results are discussed in order to define a consistent stratigraphic model of this unit and to propose a reference to all those working in the southern Apennines.

Geological framework

The Tusa Tuffite succession (Tufiti di Tusa Auct.) was originally described from the Nebrodi Mountains of north-eastern Sicily by Ogniben (1960) within the 'Sicilide Complex', as a distinctive facies characterizing the upper portion of the Polizzi Formation. This is a mixed siliciclastic/calciclastic turbidite suite which contains, in its upper part, abundant thick and coarse-grained beds rich in volcaniclastic debris. In the type-locality, this unit rests on highly tectonized varicoloured shales of Late Cretaceous to Eocene age, overthrust on the foredeep deposits of the Numidian Flysch. At the top, the Polizzi Formation-Tusa Tuffite succession is tectonically overlain by the Monte Soro Flysch (Early Cretaceous) and the Argille Scagliose Superiori (Albian to Late Cretaceous), which are the uppermost units of the Sicilide Complex. These are in turn overridden by the more internal 'Calabride Complex', cropping out in the Peloritani Mountains.

Since the work of Ogniben (1960), closely similar volcaniclastic turbidites, invariably associated with varicoloured shales and occupying the same structural position as in the Sicilian Maghrebids, were recognised in other areas of the southern Apennines (Ogniben 1969, Lentini 1979). In the whole area between the River Sinni and the Calabro/Lucano boundary (Fig. 1a), the Sicilide Complex is well exposed and allows the recognition of a geometric succession. From base to top, the following lithostratigraphic units can be recognised.

1) Lower Varicoloured Shale (Cretaceous?).

2) Monte Sant'Arcangelo member (Paleocene-Early Eocene): a series of mixed siliciclastic-calciclastic turbidites with distinctive thick (up to 15-20 m) beds of hybrid arenite followed by pinkish-reddish marl.

3) Upper Varicoloured Shale (Eocene?).

4) Tusa Tuffite (Early Oligocene).

Original stratigraphic boundaries, now obliterated by the Miocene to Recent tectonics of the Apennines, have been interpreted from bio-chronostratigraphic data and from the occurrence of the different units always in the same geometric order.

Description of the outcrops and facies analysis

The Canale Candela outcrop is one of the most spectacular in the southern Apennines, due to the quality of the exposure and to the remarkable continuity of

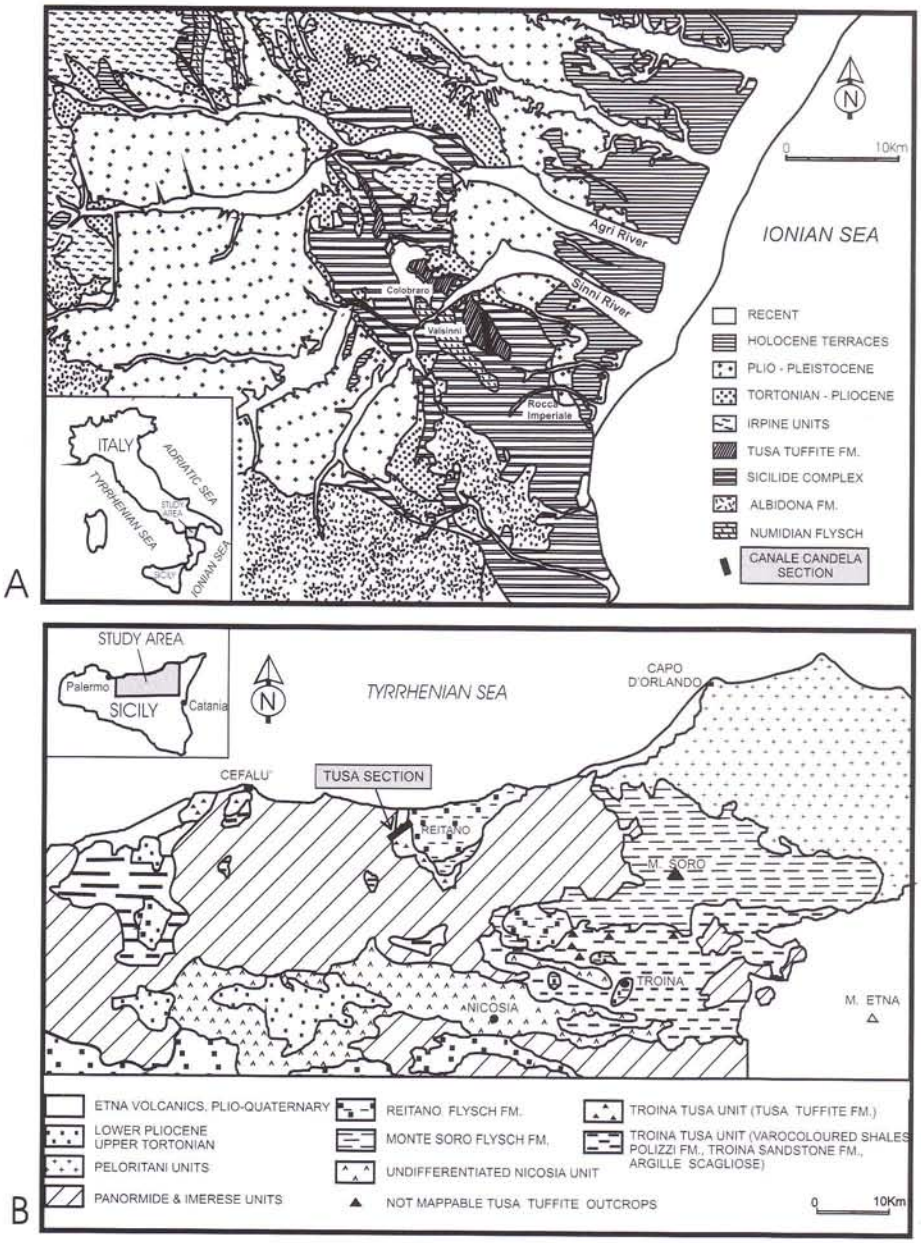

Fig. 1 (a) Geologic sketch map of the Calabro-Lucano boundary (modified after Ogniben 1969) with location of the Canale Candela section and (b) geological sketch map of north-eastern Sicily (modified after De Capoa et al. 2000) with location of the Tusa section.

the series, which is not interrupted by significant faults. The section measured, described and sampled in the present study is about 400 m thick. Coarse volcaniclastic beds are concentrated in the upper part of the succession, whereas the lower part is mostly characterized by thin to thick graded beds of fine siliciclastic, calciclastic and hybrid arenite. From base to top, the following intervals have been measured, described and sampled.

1) Chaotic varicoloured shale.

2) Regular interbedding of medium to thick-bedded siliciclastic, mixed-sediment and calciclastic turbidites (17 m). Siliciclastic turbidites are graded couplets of fine/very fine sandstone gradually passing upward to grey shale. Sandstone layers, up to 0.5 m thick, are described as F9 facies according to Mutti's (1992) classification scheme. Shale layers are generally thicker (up to 1 m), and terminate with few millimeters of greenish micaceous silty shale that is interpreted as hemipelagite. In the mixed beds, a basal division of hybrid arenite is overlain by light grey calcareous shale. Calciclastic beds are characterized by a lower division of fine bioclastic packstone grading upward to a thick white calcilutite / marl, sharply overlain by the greenish hemipelagite. Primary sedimentary features include all the spectrum of traction-plus-fallout structures classically described from diluted turbidites (Bouma 1962).

3) Same facies as above, but interbedded with very thick (up to 2 m) and medium-grained siliciclastic beds, very thick (up to 2.5 m) but fine-grained mixed and calciclastic beds, the latter often devoid of the basal packstone division, and siliciclastic TBT (19 m). Coarse siliciclastic beds display a broadly erosional base and a sharp top, which is either overlain by grey shale or directly by the next sandstone bed. The shale layer, if present, is thinner than the underlying sandstone. Beds can be described as F5/F7 sequences in Mutti's (1992) scheme. Thick fine-grained mixed and calciclastic beds are still F9 type; they are characterized by repeated sets of climbing ripples and sinusoidal laminae, the former locally showing opposite direction of migration (W to E, SW to NE and E-W).

4) Alternances of thin- to thick-bedded siliciclastic turbidites, as in point (1) (14 m). Sandstone layers are described as F9 facies. A very thick, fine grained mixed bed is found at the top of the interval.

5) Detrital cover (22 m).

6) Very thick but relatively fine-grained siliciclastic and mixed beds (13 m). Both siliciclastic and mixed beds, 2-3 m thick, are graded F8/F9 couplets, with the

F9 division characterized by large convolute laminae. Shale layers are always thicker than underlying sandstone.

7) Detrital cover (12 m).

8) Thin- to thick-bedded siliciclastic turbidites, as in point (4), interbedded with very thick and relatively fine-grained siliciclastic, mixed and calciclastic turbidites, similar to those described at point (6) (45 m). The interval contains in the middle a siliciclastic megabed, 8 m thick (4 m sandstone layer + 4 m grey shale) and two mixed megabeds, 7-8 m thick (3-4 m hybrid sandstone and 3-5 m calcareous shale/marl). All very thick beds, both siliciclastic and mixed, are described as F8/F9 couplets. In siliciclastic beds, the F9 division displays large convolute laminae, while in calciclastic beds the dominant features are climbing, nearly symmetrical ripples and megaripples in repeated sets that often show opposite migration (W to E and E to W). Some mixed beds also exhibit symmetrical truncated ripples that clearly indicate an oscillatory component in the flow.

9) Detrital cover (23 m). The top of the interval consists of poorly exposed, shale rich siliciclastic TBT (4 m thick dark shale of Critelli et al. 1990).

10) As in point (8), with interbedded very thick layers of poorly cemented, grey-greenish coarse to fine grained volcaniclastic arenite (24 m). Thick volcaniclastic beds are "slurry beds" characterized by a medial, almost chaotic interval rich in large rip-up shale and sandstone clasts. Some others, very fine grained and rich in muddy matrix, seem to be the product of cohesive sandy mudflows. Few palaeocurrent indicators (sole marks) have been recorded at the base of volcaniclastic beds, being generally oriented S-N.

11) Alternances of thin- to medium-bedded siliciclastic turbidites, as in point (4) (20 m).

12) As points (8) and (10), with occasional very thick beds of poorly cemented, grey-greenish volcaniclastic arenite with large shale clasts (17 m).

13) As point (11) (14 m).

14) As point (12) (33 m). At the top, there is a package of thick bedded, tight calcilutites that are a facies marker at a local scale.

15) Prevailing thick beds of grey-greenish, matrix-rich poorly cemented volcaniclastic arenite, coarse to fine-grained, interbedded with mud rich siliciclastic thin-bedded turbidites, often affected by slump features (23 m). A 4 m thick debris flow with boulders of fine siliciclastic sandstone in a grey silty matrix is found at 12 m from the bottom of the interval. Volcaniclastic beds are generally coarse, ungraded and matrix-supported, with large floating shale clasts.

16) Thick (2 m) mixed-sediment bed showing a lower interval (1.5 m) of graded, coarse to fine hybrid arenite sharply overlain by an upper interval (0.5 m) of white marl. The arenite division is characterized by thick horizontal traction-carpet laminae (F7 facies) followed by thick to thin truncated sinusoidal laminae that resemble the hummocky-cross stratification of storm layers in shelf settings.

17) As point (15), with some thick mixed siliciclastic-marly beds concentrated in the middle of the interval (27 m).

18) Medium- to fine-grained, light-coloured, very tightly cemented arenite, rich in grey shale clasts (3 m). This bed seems to be compositionally different from other volcaniclastic arenites and could represent a stratigraphical marker.

19) As points (10), (12) and (14), for a total thickness of 49 m. Medium grained volcaniclastic beds, thick to very thick, are usually of the "slurry" type. A few are not graded and rich in muddy matrix.

20) Prevailing thin-bedded, mud-rich siliciclastic turbidites with two very thick bedded (2-3 m each), graded hybrid arenite/marl beds, similar to those at point (8) (21 m).

21) Chaotic varicoloured shale with packages of thin siliciclastic and mixed-sediment turbidites affected by slump deformations.

As far as the interpretation of facies and dynamics of the system are concerned, field data allow some inter-

PLATE 1

Facies in the lower (a, b, c) and upper (d, e, f) portion of the Tusa Tuffite Formation, Canale Candela section.
a) Top of a calciclastic megabed characterized by repeated sets of horizontal traction-plus-fallout laminae, ripples and sinusoidal laminae, indicating a flow with pulsing behaviour. Palaeoflow direction from SW to NE (arrow). b) Mixed-sediment bed showing horizontal laminae (hl) overlain by truncated nearly symmetrical ripples (tsr). These structures indicate superimposition of an oscillatory component on a unidirectional flow. c) Mixed-sediment bed showing horizontal laminae (hl) overlain by repeated sets of sinusoidal laminae (sl) with convolute features (cl). These structures can be explained either as water-escape features due to high deposition rate, or as disrupted features generated by high-energy reflection flows ("bores") propagating in a backwards direction after the forward flow has collided with an obstacle. In both cases, an unstable flow with pulsing behaviour is envisaged. d) Panoramic view of the upper part of the Tusa Tuffite at Canale Candela. Major resistant beds are matrix-rich volcaniclastic turbidites, more than 5 m thick (v). These beds were deposited by high-density immature flows that were not able to sort the different grain sizes in the downslope motion. In the middle of the cliff, a dark-coloured, 5 m thick bed of the slurry type can be seen (sl). e) The top of the outcrop section at Canale Candela. A three m thick, matrix-rich volcaniclastic bed (v) is shown in the middle of the outcrop. f) The top of a thick volcaniclastic bed of the slurry type. The chaotic slurry division (sl) is overlain by a thin (10 cm) cemented F9 with convolute laminae and a thin (about 20 cm) shale layer (sh). The paucity of fine sediment in the volcaniclastic beds is explained by the deposition of poorly sorted sandstone facies from dense immature flows.


SW
NE
a

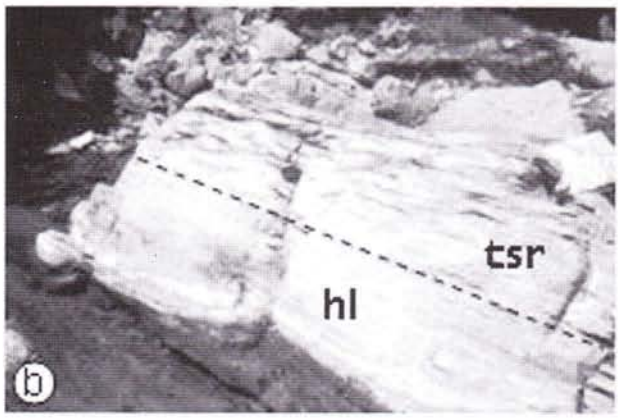
tsr
hl
b

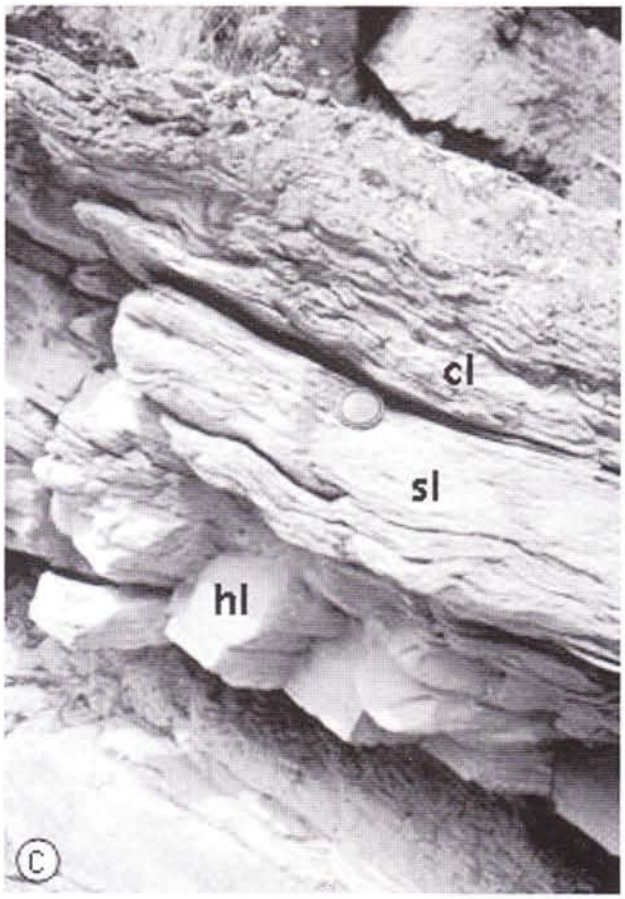
cl
sl
hl
c


v
v
sl
v
d


v
e

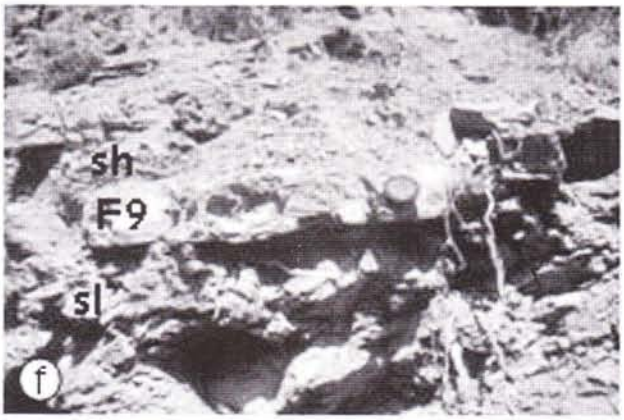
sh
F9
sl
f

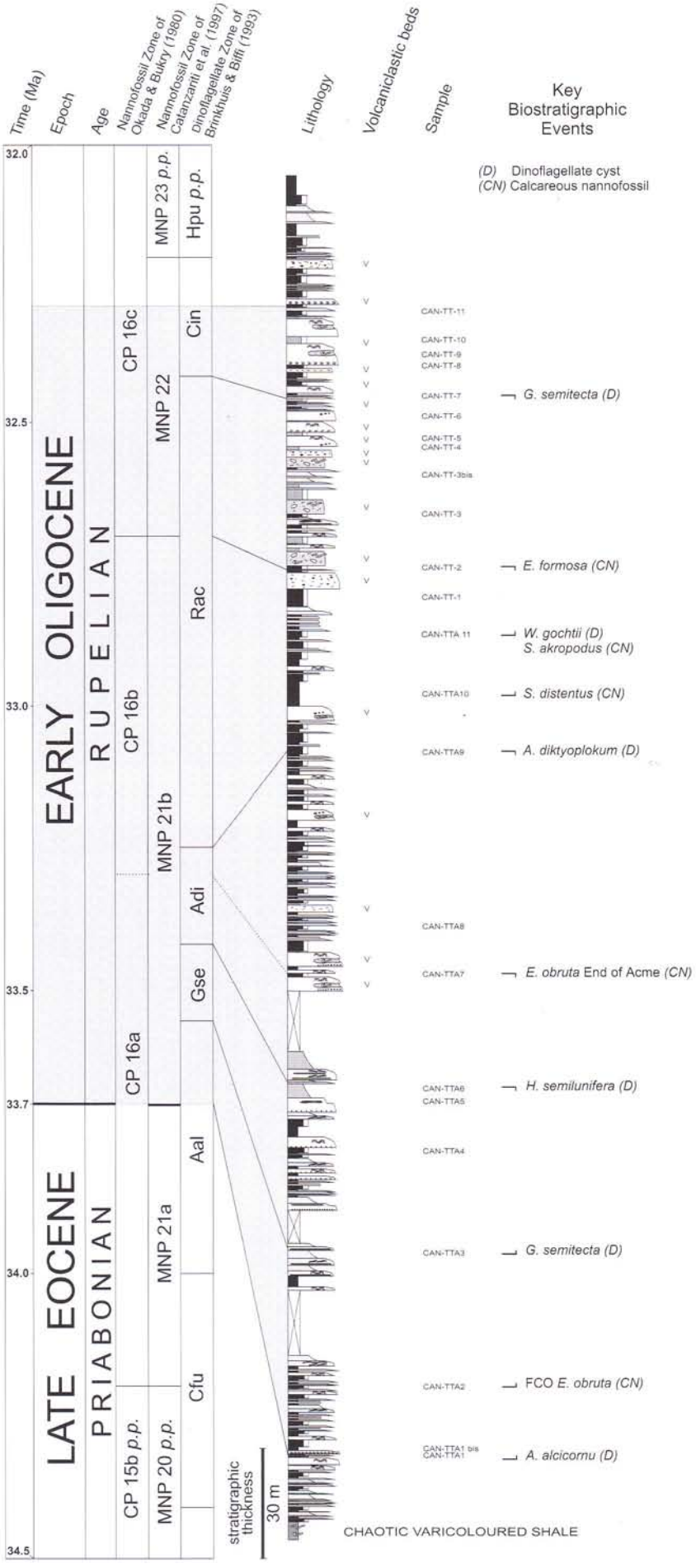
Time (Ma)
Epoch
Age
Nannofossil Zone of Okada & Bukry (1980)
Nannofossil Zone of Catanzariti et al. (1997)
Dinoflagellate Zone of Brinkhuis & Biffi (1993)
Lithology
Volcaniclastic beds
Sample
Key Biostratigraphic Events
(D) Dinoflagellate cyst
(CN) Calcareous nannofossil
LATE EOCENE
EARLY OLIGOCENE
PRIABONIAN
RUPELIAN
CP 15b p.p.
CP 16a
CP 16b
CP 16c
MNP 20 p.p.
MNP 21a
MNP 21b
MNP 22
MNP 23 p.p.
Cfu
Aal
Gse
Adi
Rac
Cin
Hpu p.p.
32.0
32.5
33.0
33.5
33.7
34.0
34.5
CAN-TT-11
CAN-TT-10
CAN-TT-9
CAN-TT-8
CAN-TT-7
CAN-TT-6
CAN-TT-5
CAN-TT-4
CAN-TT-3bis
CAN-TT-3
CAN-TT-2
CAN-TT-1
CAN-TTA 11
CAN-TTA10
CAN-TTA9
CAN-TTA8
CAN-TTA7
CAN-TTA6
CAN-TTA5
CAN-TTA4
CAN-TTA3
CAN-TTA2
CAN-TTA1 bis
CAN-TTA1
G. semitecta (D)
E. formosa (CN)
W. gochtii (D)
S. akropodus (CN)
S. distentus (CN)
A. diktyoplokum (D)
E. obruta End of Acme (CN)
H. semilunifera (D)
G. semitecta (D)
FCO E. obruta (CN)
A. alcicornu (D)
stratigraphic thickness
30 m
CHAOTIC VARICOLOURED SHALE

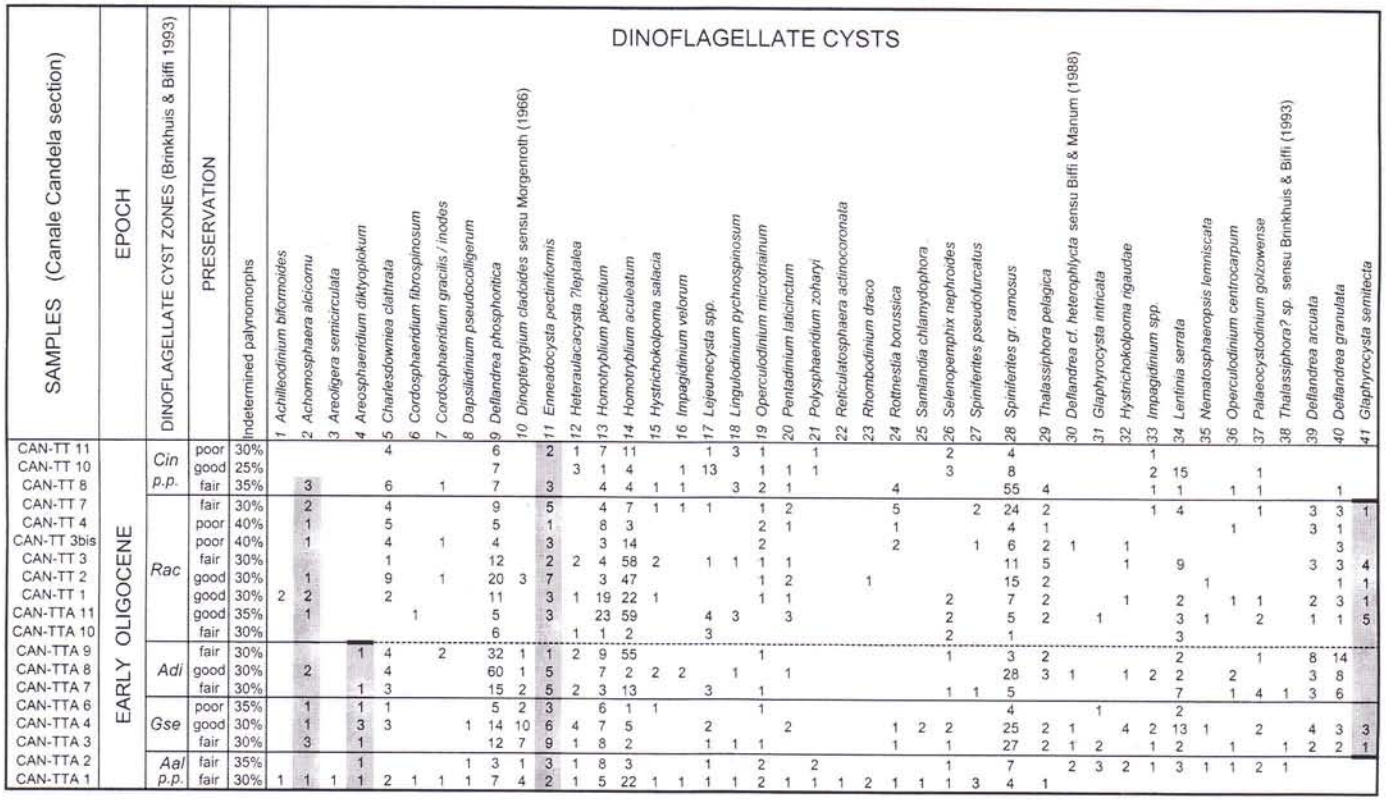

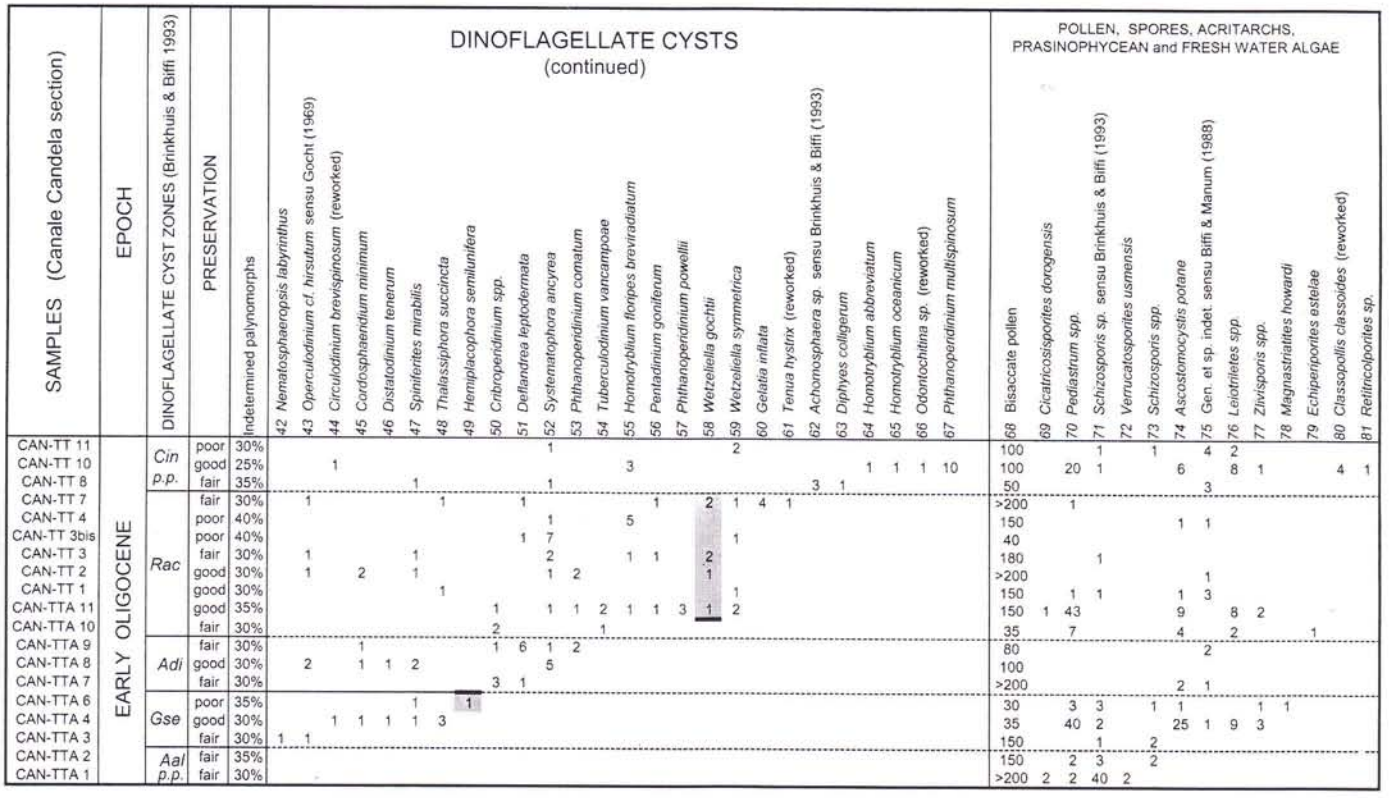

Fig. 2 Stratigraphic log of the Tusa Tuffite Formation at the Canale Candela section showing schematic lithology, position of the studied samples, key biostratigraphic events and corresponding biostratigraphies. Timescale after Berggren et al. (1995).

Fig. 3 Quantitative distribution-chart of the palynomorphs recovered from the Canale Candela section, ordered according to first occurrences and plotted using abundances obtained from a count of a single slide. Samples missing with respect to progressive numbering were collected from palynologically barren sandstones for petrographic investigations. Following the dinoflagellate cyst zonation scheme of Brinkhuis & Biffi (1993), key taxa and key events are highlighted. Vertical scale is not proportional to stratigraphic thicknesses.

a

MNP 22	BIOZONES (Catanzariti et al. 1997)
TUS B-15 … TUS B-1	SAMPLES Tusa section
F … barren	TOTAL ABUNDANCE
G … barren	PRESERVATION
c … r	1 *Coccolithus pelagicus*
c … r	2 *Dictyococcites bisectus*
rr … r	3 *Discoaster gr. tanii*
r … rr	4 *Ericsonia formosa*
s/c … r/s	5 *Ericsonia obruta*
s … rr	6 *Lanternithus minutus*
s … rr	7 *Reticulofenestra daviesii*
c/a … c/a	8 Small Placoliths
s … s	9 *Sphenolithus moriformis*
s … r	10 *Sphenolithus predistentus*
s … s/c	11 *Zygrablithus bijugatus*
r … s/c	12 *Zygrablithus bijugatus* (distal view)
r … rr	13 *Discoaster saipanensis*
r … rr	14 *Discoaster gr. deflandrei*
r/s … r	15 *Helicosphaera compacta*
r/s … rr	16 *Reticulofenestra umbilicus/hillae*
r … rr	17 *Helicosphaera bramlettei*
s/c … rr	18 *Ismolithus recurvus*
r … r	19 *Rhabdosphaera spp.*
rr … r/s	20 *Sphenolithus akropodus*
r … r	21 *Helicosphaera dinesenii/hezenii*
r … r	22 *Reticulofenestra spp.* (10-12 microns)
rr … rr	23 *Coccolithus eopelagicus*
r/s … r/s	24 *Sphenolithus predistentus/distentus*
r … r/s	25 *Sphenolithus distentus*
rr … r	26 *Helicosphaera reticulata*
rr	27 *Chiasmolithus oamaruensis*
	28 Cretaceous Reworking

b

MNP 21a	MNP 21b	MNP 22	BIOZONES (Catanzariti et al. 1997)
CAN TT - 11 … CAN TTA - 1			SAMPLES Canale Candela section
F … barren			TOTAL ABUNDANCE
G … barren			PRESERVATION
x	0,1	0,8 10,5	1 *Coccolithus eopelagicus*
10,3	10,3	10,1 11,5 10 8	2 *Coccolithus pelagicus*
x		0,4	3 *Chiasmolithus oamaruensis*
0,3		0,9	4 *Cribrocentrum reticulatum* (small)
		4,5 5,1 3,8 6,5 5,5	5 *Dictyococcites bisectus*
		3	6 *Discoaster gr. barbadiensis*
		0,8 1,2 1	7 *Discoaster gr. tanii*
		0,3	8 *Discoaster saipanensis*
	3	0,4 2,1 0,7 2 0,9 11,2 0,6 1,5	9 *Ericsonia formosa*
		0,7 2,3 2,9 2,8 2,5 0,8	10 *Ericsonia obruta*
	0,2	1,6 1,3 1,2 1,9	11 *Ericsonia spp.* (small)
		2,3 4,8	12 *Helicosphaera spp.*
		4,3	13 *Helicosphaera bramlettei*
		6,2 1,2 1,9	14 *Helicosphaera compacta*
		0,4	15 *Ismolithus recurvus*
		0,2	16 *Lanternithus minutus*
		0,3 0,8 0,4 0,4	17 *Reticulofenestra daviesii*
		0,8 2,3	18 *Reticulofenestra umbilicus/hillae*
		54,6 5	19 Small Placoliths
		0,2	20 *Sphenolithus moriformis*
		0,8	21 *Sphenolithus predistentus*
		1,8 1,5	22 *Toweius spp.*
		0,4	23 *Zygrablithus bijugatus*
		0,2	24 *Zygrablithus bijugatus* (distal view)
		0,9	25 *Helicosphaera intermedia/euphratis*
		0,6	26 *Helicosphaera dinesenii/hezenii*
		0,5	27 *Helicosphaera reticulata*
		0,3	28 *Discoaster gr. deflandrei*
		0,9	29 *Sphenolithus distentus*
		0,4	30 *Sphenolithus radians*
		0,3	31 *Rhabdosphaera spp.*
		0,7	32 *Sphenolithus predistentus/distentus*
		0,5	33 *Helicosphaera lophota*
		0,7	34 *Traversopontis spp.*
		0,3	35 *Sphenolithus akropodus*
		3,2 1,1	36 *Reticulofenestra spp.* (10-12 microns)
		1,2 5,1 2,3 2,3	37 Cretaceous Reworking
		0,8 1,2 0,4 0,8	38 Paleogene Reworking
			ADDITIONAL EVENTS

E. obruta End of Acme ?

S. distentus and related species

Total Abundance: A = > 30 spec./field, F = 11-30 spec./ field, C = 2-10 spec./ field, S= 1 spec./ field, R = < 1 spec./ field

Preservation: P= poor, M= moderate; G= good

Specific Abundance: a = > 1 spec./field, c = 1 spec./ 2-10 fields, s = 1 spec./ more than 10 fields, r = some spec./ more than 100 fields, rr = 1 spec. during the count, x= species undetected during the count.

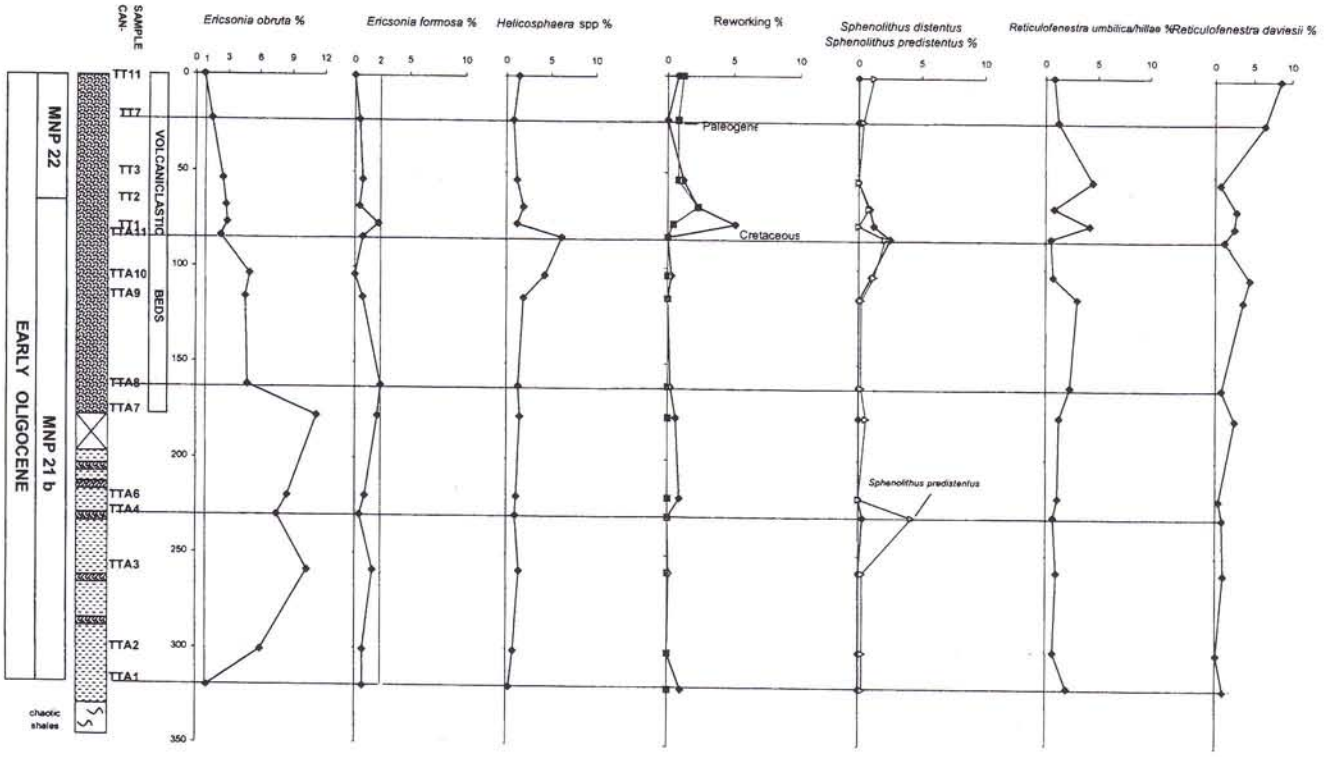

Fig. 4c Quantitative distribution patterns of selected nannofossil taxa in the Canale Candela section. Abundances are expressed in percentages of the overall assemblages. The FCO of *Ericsonia obruta* and the LO of *Ericsonia formosa* are defined according to the quantitative criteria proposed by Catanzariti et al. (1997). See text for discussion.

pretation. In the lower part of the Tusa Tuffite, both siliciclastic, mixed and calciclastic beds are mostly described as F8/F9 couplets or F9 facies, with reference to Mutti's (1992) classification scheme. A few thick, coarse-grained poorly graded siliciclastic beds with sharp top and almost devoid of shale divisions are ascribed to the F5 facies. The bulk of sediment has thus been emplaced by relatively diluted and high-efficiency flows, able to cover large distances from the sediment source and to sort laterally the different granulometric populations. However, major beds display features that are not part of the classical Bouma (1962) sequence for diluted turbidites. Such features include:

· repeated sets of horizontal, ripple-drift and sinusoidal laminae, often showing opposite direction of migration;

· truncated nearly symmetrical ripples/megaripples, sometimes resembling hummocky cross stratification (HCS) of shallow-water environments;

· large asymmetrical convolute laminae, in repeated sets.

These structures appear to be characteristic of unstable flows that experience interaction (reflection/deflection) with the basin margins or with intra-basinal uplifts. Repeated sets of ripples with opposite polarity have been described by Pickering & Hiscott (1985) from the Ordovician Cloridorme Formation of Quebec, and interpreted as generated from flow reflection at basin margins. Oscillatory features (symmetrical ripples/megaripples) are here interpreted as the result of weak "type A" bores (reflected flows propagating as trains of solitary waves; Edwards et al. 1994). Convolute laminae are classically considered dewatering features due to rapid deposition from dilute turbulent suspensions via traction-plus-fallout processes. In this case, their occurrence in very thick beds in alternance with less disrupted sinusoidal laminae may indicate repeated perturbations of the main flow, possibly due to strong "type C" bores (reflected flows propagating as density currents having the characteristics of the parent forward flows; Edwards et al. 1994).

All these observations suggest large-volume diluted flows confined (ponded) in a basin that was relatively small if compared to the average flow volume. In this view, the majority of palaeocurrent indicators, showing

Fig. 4 (a) Quantitative distribution-chart of calcareous nannofossils recovered from the Canale Candela section and (b) qualitative distribution-chart of calcareous nannofossils recovered from the Tusa section, ordered according to first occurrences. Samples missing with respect to progressive numbering were collected from sandstones for petrographic investigations. Key taxa and key events are highlighted. Vertical scale is not proportional to stratigraphic thicknesses.

W-E and E-W flow directions, could only reflect locations of the basin margins, rather than a true position of sediment sources.

In the upper part of the series, thick volcaniclastic beds dominate the facies assemblage. Volcaniclastic beds are basically of three types:

1. Thick (more than 2 m), coarse-grained, poorly graded, poorly sorted (matrix-rich). These beds were deposited by dense immature flows that were not able to sort grain size classes downslope. Flows with such characteristics are generally not able to travel a large distance from their sources, because internal frictional forces lead to a rapid loss of energy. Thus, a sediment source area very close to the basin is envisaged. Most of these beds are also capped by a thin F9/shale division, which probably represents the diluted portion of the flow (turbulent cloud) that did not overtake the deposition area of coarse sediment because of ponding.

2. Thick, graded beds with a chaotic (slurry) division overlain by laminated F9 facies. These beds are interpreted as deposited by medium-density flows that were able to travel for longer distances and thus to experience interaction with the basin margins. Strong reflection bores ("type C" of Edwards et al. 1994) developed upon collision of the flow with obstacles, would have been able to entrain the sediment just deposited by the forward parent flow, giving rise to the chaotic slurry division.

3. Thick, matrix-supported with sharp base, sharp top and outsize shale and sandstone clasts. These beds seem to be the product of the "freezing" of cohesive debris flows/mudflows.

In conclusion, a confined oversupplied basin is envisaged for both the lower and the upper part of the Tusa Tuffite Formation at Canale Candela. No major changes in the basin size and shape are directly inferred from the appearance of volcaniclastic beds, which only mark the onset of a source of volcanic debris close to, but outside the basin. The appearance of the volcanic debris is a sudden phenomenon but it is not coupled with a de-activation of other sediment sources, as normal siliciclastic and mixed/calciclastic beds are still present in the upper portion of the Tusa Tuffite Formation.

Biostratigraphic analyses: material and methods

Twenty samples of shale collected from the Canale Candela section (Calabro-Lucano boundary, southern Italy, Fig. 1a) and sixteen samples of shale collected from the Tusa section (northern Sicily, Fig. 1b) were processed and analysed for palynomorphs and calcareous nannofossils. Sample positions at the Canale Candela section are shown in Fig. 2 with the lithostratigraphy, the key biostratigraphic events and corresponding stratigraphy.

Palynology. The standard processing technique was performed in the ENI-Agip Division laboratories and involved cold chemical treatment of 15g of sediment with hydrochloric acid (HCl 36%) to remove the calcareous fraction and with hydrofluoric acid (HF 40%) to remove the silicates, heavy liquid separation with $ZnCl_2$, sieving with 250µm and 15µm meshes, and centrifuging to concentrate the residues. No oxidation was required. Two slides were prepared for each sample using part of the residues greater than 15µm. Optical adhesive produced by Norland Inc. was used as mounting medium.

The analytical results are shown in the quantitative distribution-chart (Fig. 3) plotted with absolute abundances obtained from a count of a single slide. The second slide of each sample was also examined to check for the presence of additional taxa. The analytical method applied herein is not strictly quantitative (see Brinkhuis 1994), since all the shale samples prepared were analysed and used for palynostratigraphic evaluation, independently on the overall fossil recovery and without using percentages.

Light photomicrographs were taken using a Zeiss Axioplan microscope and interference-contrast illumination (Plates 2, 3). The taxonomic allocation and authorship of dinoflagellate cyst species listed in Appendix below follow Williams et al. (1998). All the slides examined in this study are housed with a progressive numbering from A17121 to A17158 in the palynological collection at the Stratigraphic Dept. (LABO-STIG) of ENI S.p.A.-Agip Division, San Donato Milanese, Italy.

Calcareous Nannofossils. Rock samples were mechanically disaggregated and smeared onto slides following the standard preparation method, without apply-

PLATE 2

Dinoflagellate cysts and prasinophycean algae from the Tusa Tuffite Formation, Canale Candela section. All figures x 500.

(1) *Wetzeliella symmetrica*, sample CAN-TTA 11, slide A17158. (2) *Charlesdowniea clathrata*, sample CAN-TT 4, slide A17129. (3) *Rhombodinium draco*, sample CAN-TTA 1, slide A17139. (4) *Wetzeliella gochtii*, sample CAN-TTA 11, slide A17157. (5) *Thalassiphora*? sp. of Brinkhuis & Biffi (1993), sample CAN-TTA 2, slide A17141. (6) *Heteraulacacysta ?leptalea*, sample CAN-TTA 4, slide A17145. (7) *Achomosphaera* sp. sensu Brinkhuis & Biffi (1993), sample CAN-TT 8, slide A17133. (8) *Achomosphaera alicornu*, sample CAN-TTA 8, slide A17152. (9) *Areosphaeridium diktyoplokum*, sample CAN-TTA 2, slide A17142. (10) *Operculodinium* cf. *hirsutum* sensu Gocht (1969), sample CAN-TTA 8, slide A17152. (11) *Enneadocysta pectiniformis*, sample CAN-TTA 4, slide A17145. (12) *Schizosporis* sp. of Brinkhuis & Biffi (1993), prasinophycean algae, sample CAN-TTA 1, slide A17140. (13) *Schizosporis* spp., prasinophycean algae, sample CAN-TTA 2, slide A17141.

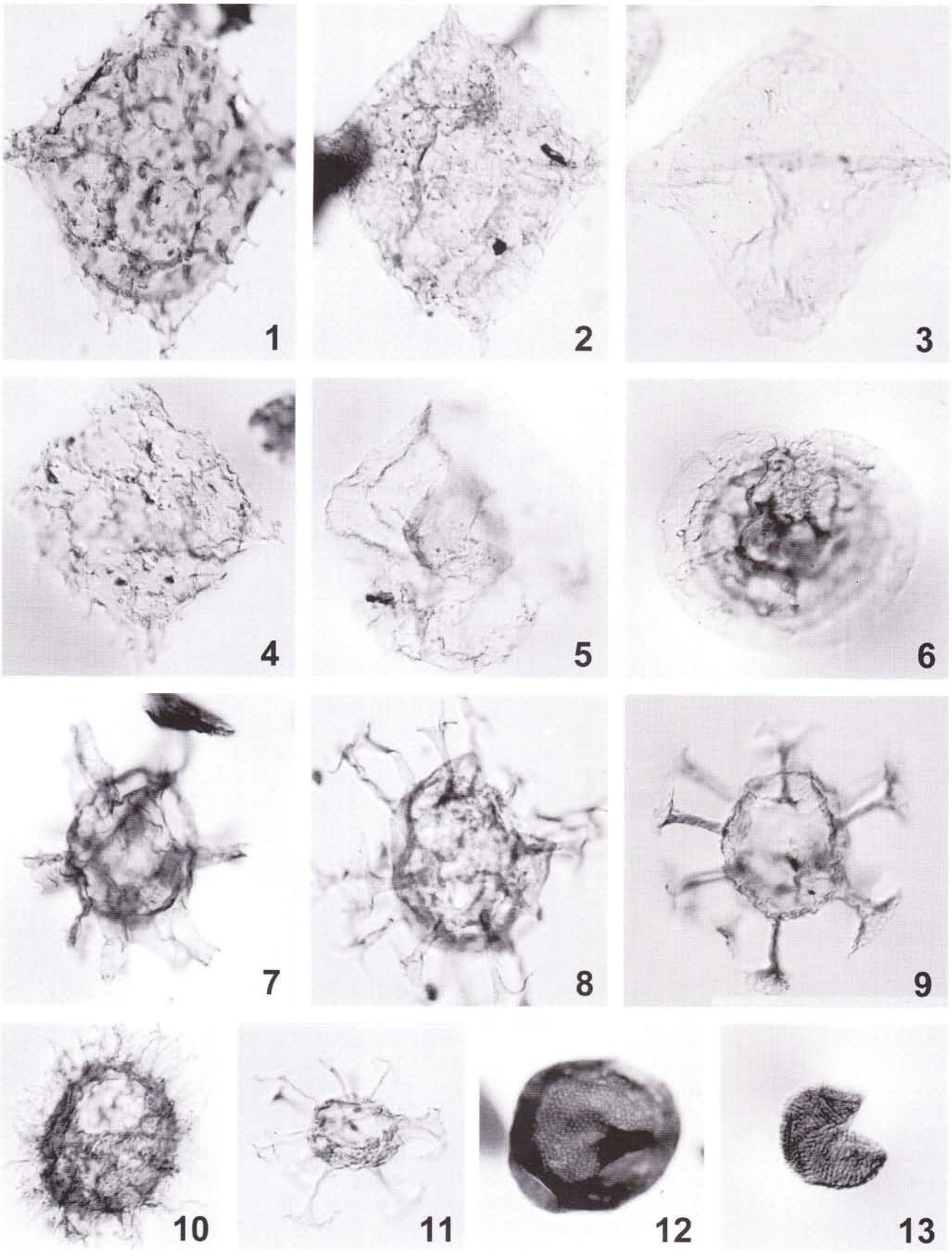
1
2
3
4
5
6
7
8
9
10
11
12
13

ing any concentration technique in order to retain the original nannofloral assemblage. Analyses were carried out with a Zeiss Axioplan microscope at x1000 and x1250 magnifications.

A qualitative analysis was carried out on samples from the Canale Candela section in order to evaluate nannofossil abundance, preservation and taxonomic composition of the assemblages. A quantitative approach was then applied in order to assess abundance variations of index species (fig 4c). A 300 specimens count, aimed at evaluating the general composition of the nannofossil assemblage, pointed out the dominance of "Small placoliths" (small *Dictyococcites* spp., small reticulofenestrids, *Cyclicargolithus floridanus*) making up 70-80% of the total assemblage; hence, in order to assess abundance variations of other species, the count was extended up to 700/800 specimens per slide. Analytical results are shown in Fig. 4a. For samples CAN TT 4 and CAN TT 8 only semiquantitative data are reported owing to the scarcity of the nannofossil content. In the samples from Tusa (northern Sicily) nannofossils are scarce in the lower part of the section (probably due to unfavourable lithology), whereas they are more frequent in the upper part; semiquantitative data only, derived from the richest samples in the upper part of the section, are reported in the distribution-chart (Fig. 4b).

Biostratigraphy.

Palynomorph biostratigraphy of the Canale Candela section

All samples contained diverse and fairly well-preserved palynological assemblages consisting of dinoflagellate cysts, acritarchs, pollen, spores, prasinophycean and fresh water algae in fluctuating relative abundances. Microforaminiferal linings occur abundantly in the lowermost part of the section (CAN-TTA 1 - CAN-TTA 4) and in trace amounts from sample CAN-TTA 6 upwards. Reworked dinoflagellate cysts, identified by their known Cretaceous stratigraphic ranges, are rare and also plotted in the distribution-chart (Fig. 3).

This study is mainly focused on dinoflagellate cysts, as they provide an efficient tool in order to determinate the precise biostratigraphy of the section. However, the local biostratigraphic importance of selected pollen and prasinophycean algae is also pointed out. The dinoflagellate cyst zonation scheme established by Brinkhuis & Biffi (1993) (Fig. 5) at Massignano (central Italy), at the Global Stratotype Section and Point (GSSP) for the Eocene/Oligocene (E/O) boundary, has been successfully used as a framework for the stratigraphic interpretation of the cyst distribution in the Tusa Tuffite Formation. All the key dinostratigraphic events, defining the four zones of Brinkhuis & Biffi (1993) in the lowermost Oligocene, were in fact recorded at the Canale Candela section in the same sequence of occurrence. It is worthwhile mentioning that, in addition to the occurrences of key taxa herein discussed, also the overall composition of the palynological assemblages recovered in this study is very similar to that previously documented from other lowermost Oligocene sections of the central Mediterranean area (Biffi & Manum 1988; Brinkhuis & Biffi 1993; Brinkhuis 1994; Torricelli 2000).

The co-occurrences in the basal sample of the Canale Candela section of the zonal marker *Achomosphaera alcicornu* and of *Areosphaeridium diktyolplokum*, combined with the absence of *Glaphyrocysta semitecta* (that first occurs in sample CAN-TTA 3), allow the recognition of the Aal Zone of Brinkhuis & Biffi (1993) that spans the E/O boundary in the GSSP at Massignano. More in detail, following also the chronostratigraphic calibration provided by calcareous nannofossils, samples CAN-TTA 1 and 2 are likely representative of the upper portion of the Aal Zone, earliest Oligocene in age. Both the high abundance of bisaccate pollen (conifers), that was shown to increase across the E/O transition as a response to a change in climate towards cooler conditions (Brinkhuis & Biffi 1993), and the abrupt decrease in abundance of prasinophycean algae referable to *Schizosporis* sp. sensu Brinkhuis & Biffi (1993) in the samples above CAN-TTA 1, support this age assessment.

PLATE 3

Dinoflagellate cysts from the Tusa Tuffite Formation, Canale Candela section. All figures x 500.
(1) *Samlandia chlamydophora*, sample CAN-TTA 1, slide A17140. (2-3) *Rottnestia borussica*, sample CAN-TT 7, slide A17131, same specimen in high and low focus. (4) *Phthanoperidinium multispinosum*, sample CAN-TT 10, slide A17136. (5) *Hystrichokolpoma salacia*, sample CAN-TTA 8, slide A17152. (6) *Glaphyrocysta semitecta*, sample CAN-TTA 4, slide A17145. (7) *Impagidinium velorum*, sample CAN-TTA 8, slide A17151. (8) *Thalassiphora succincta*, sample CAN-TTA 4, slide A17146. (9) *Nematosphaeropsis lemniscata*, sample CAN-TTA 2, slide A17141. (10) *Areoligera semicirculata*, sample CAN-TTA 1, slide A17140. (11) *Enneadocysta pectiniformis*, sample CAN-TTA 8, slide A17152. (12) *Homotryblium aculeatum*, sample CAN-TTA 4, slide A17145. (13) *Areosphaeridium diktyoplokum*, operculum, sample CAN-TTA 4, slide A17145. (14) *Lentinia serrata*, sample CAN-TTA 4, slide A17145. (15) *Lentinia serrata*, sample CAN-TT 10, slide A17136. (16) *Lejeunecysta* spp., sample CAN-TT 10, slide A17135. (17) *Deflandrea granulata*, sample CAN-TTA 4, slide A17145. (18) *Deflandrea* cf. *heterophlycta* sensu Biffi and Manum (1988), sample CAN-TTA 2, slide A17142. (19) *Deflandrea arcuata*, sample CAN-TTA 11, slide A17158. (20) *Deflandrea* spp., sample CAN-TTA 4, slide A17145.

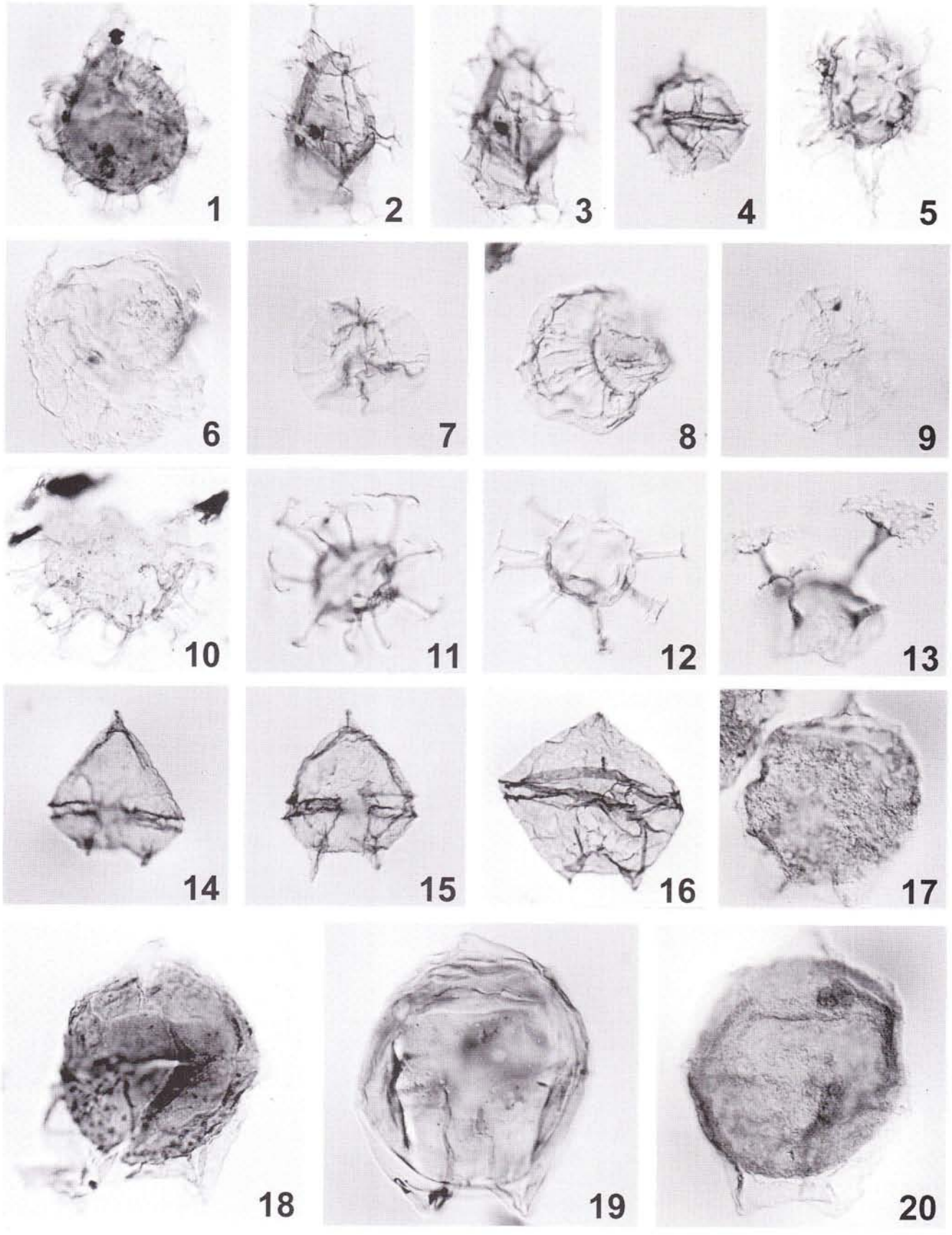
1
2
3
4
5
6
7
8
9
10
11
12
13
14
15
16
17
18
19
20

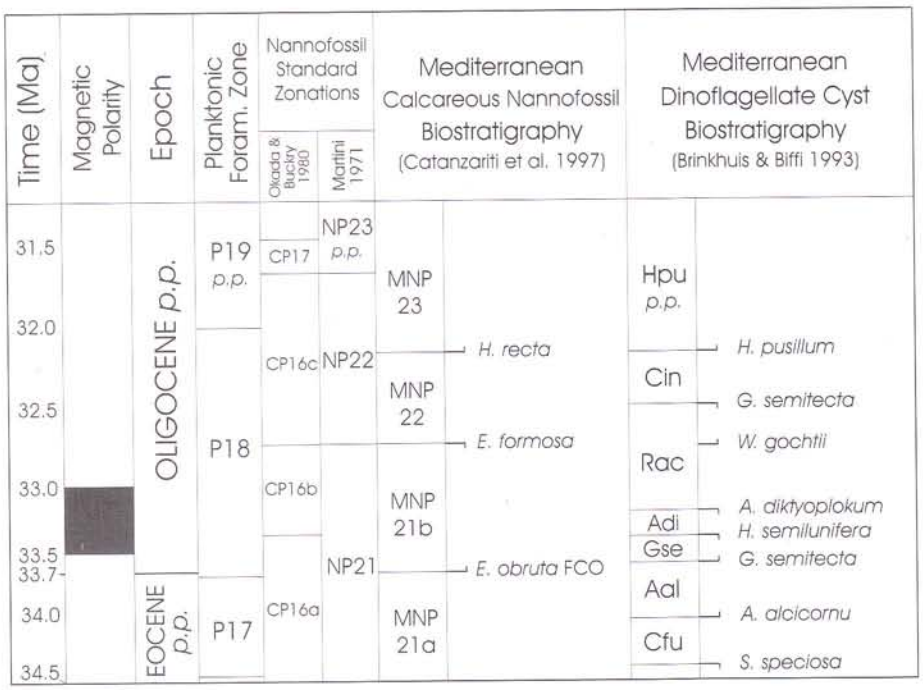

Fig. 5 Latest Eocene-earliest Oligocene dinoflagellate cyst and calcareous nannofossil zonations for the central Mediterranean adapted from Brinkhuis & Biffi (1993) and Catanzariti et al. (1997), with schematic composite diagram of correlatable bio- and magnetostratigraphies. CP = standard nannofossil zones (after Okada & Bukry 1980); NP = standard nannoplankton zones (after Martini 1971); PF = standard planktonic foraminifer zones (after Blow 1969).

The identification of the Gse Zone of Brinkhuis & Biffi (1993) relies on the lowest occurrence of the zonal marker *G. semitecta* in sample CAN-TTA 3 and on the occurrence of *Hemiplacophora semilunifera* in sample CAN-TTA 6. Moreover, the relative decrease in abundance of bisaccate pollen (conifers) recorded in samples CAN-TTA 4 and 6 perfectly fits with the short-termed relative warm interval inferred by Brinkhuis & Biffi (1993) within the Gse Zone.

The lack of *H. semilunifera* above sample CAN-TTA 6, the marked increase of bisaccate pollen in sample CAN-TTA 7 and the highest occurrence of *A. diktyolplokum* in sample CAN-TTA 9 allow the recognition of the Adi Zone. Consistently with data both from central Italy (Brinkhuis & Biffi 1993) and from northeastern Italy (Brinkhuis 1994), the high relative abundance and morphological diversity among specimens belonging to the genus *Deflandrea* are further distinctive elements of the dinoflagellate cyst assemblages in this interval.

Again following Brinkhuis & Biffi (1993), the section between the highest occurrence of *A. diktyolplokum*, recorded in sample CAN-TTA 9, and the highest occurrence of *G. semitecta*, recorded in sample CAN-TT 7, can be assigned to the Rac Zone. This zonal attribution is supported also by the lowest occurrence of *Wetzeliella gochtii* in sample CAN-TT A 11, since this event was shown to occur within the Rac Zone both in central Italy (Brinkhuis & Biffi 1993) and in northern Tunisia (Torricelli 2000, Torricelli & Biffi 2001).

Whereas the base of the Cin Zone, placed above the Rac Zone, was defined by the highest occurrence of *G. semitecta*, its top remained undefined in the paper by Brinkhuis & Biffi (1993), because the section available to those authors did not reach high enough into the Oligocene. Accordingly, in publishing the composite dinoflagellate zonation scheme for the Oligocene of the central Mediterranean, Wilpshaar et al. (1996) provided an emendation of the Cin Zone of Brinkhuis & Biffi (1993), and its top was defined by the lowest occurrence of *Hystrichokolpoma pusillum*. Since in this study *H. pusillum* was not encountered, the three highest samples

PLATE 4

Calcareous nannofossils from the Tusa Tuffite Formation, Canale Candela section. All figures x 1250.

(1) *Ericsonia formosa*, sample CAN-TTA 2. (2-3) *Dictyococcites bisectus*, sample CAN-TTA 2. (4) *Istmolithus recurvus*, sample CAN-TTA 1. (5) *Reticulofenestra umbilicus/hillae*, sample CAN-TTA 1. (6) *Coccolithus eopelagicus*, sample CAN-TTA 8. (7) *Ericsonia obruta*, sample CAN-TTA 7. (8) *Ericsonia obruta*, sample CAN-TTA 3. (9) *Discoaster* gr. *barbadiensis*, sample CAN-TTA 11. (10) *Discoaster* gr. *tanii*, sample CAN-TTA 11. (11-12) *Discoaster saipanensis*, sample CAN-TTA 4. (13-14) *Discoaster* gr. *deflandrei*, sample CAN-TTA 11. (15) *Rhabdosphaera pinguis*, sample CAN-TTA 10. (16-17) *Helicosphaera compacta*, sample CAN-TTA 1. (18-19) *Helicosphaera reticulata*, sample CAN-TTA 8. (20) *Helicosphaera bramlettei*, sample CAN-TTA 7. (21) *Helicosphaera compacta*, sample CAN-TTA 11. (22) *Lanternithus minutus*, sample CAN-TTA 10. (23) *Reticulofenestra daviesii*, sample CAN-TTA 1. (24) *Ericsonia obruta*, sample CAN-TTA 8. (25) *Sphenolithus predistentus*, sample CAN-TTA 11. (26) *Sphenolithus predistentus*, sample CAN-TTA 2. (27) *Sphenolithus predistentus*, sample CAN-TTA 11. (28-29) *Sphenolithus akropodus*, sample CAN-TTA 10. (30) *Sphenolithus distentus*, sample CAN-TTA 4.

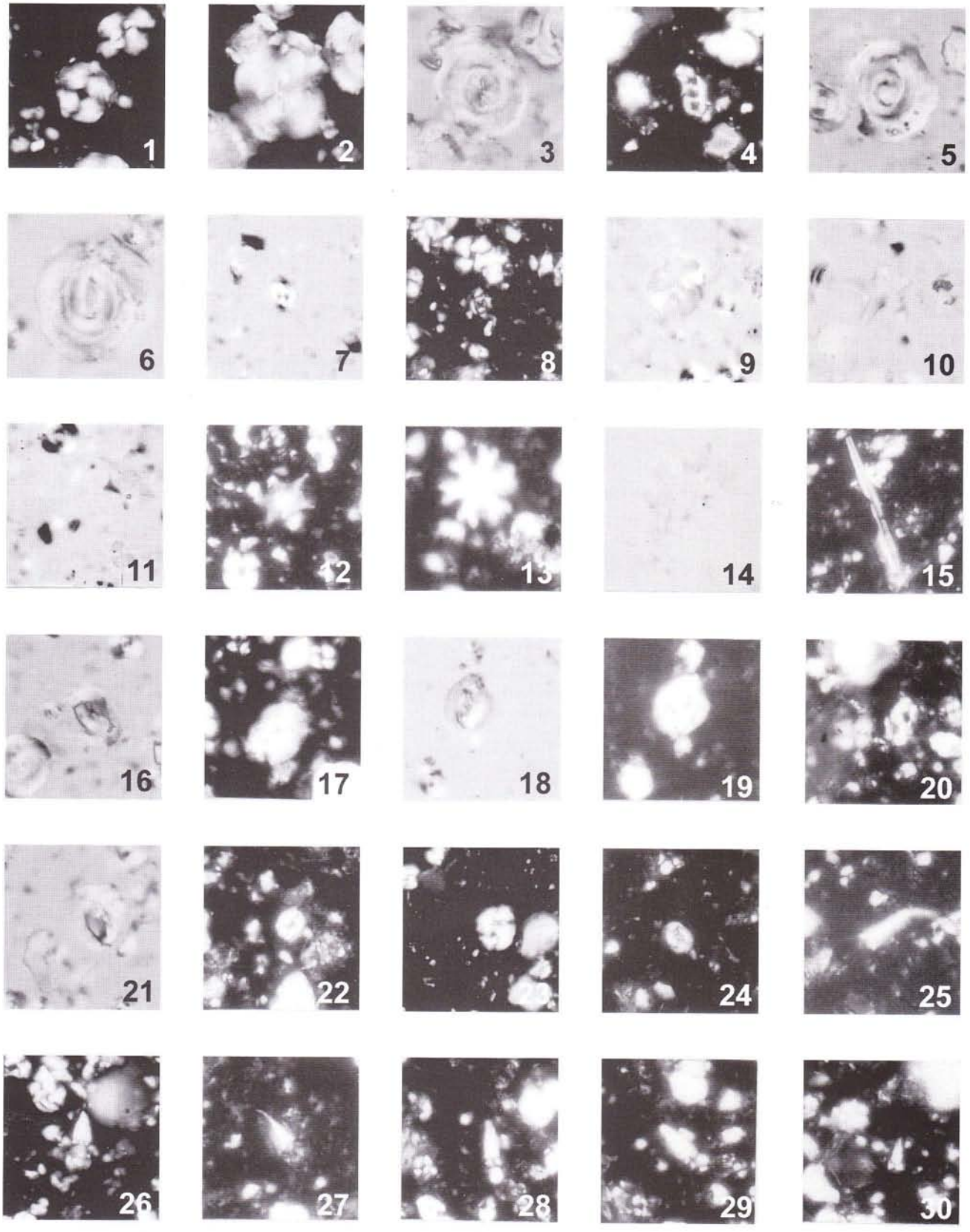
1
2
3
4
5
6
7
8
9
10
11
12
13
14
15
16
17
18
19
20
21
22
24
25
26
27
28
29
30

of the Canale Candela section (CAN-TT 8, 10, 11) are referable to the Cin Zone of mid-Early Oligocene age. Consistently with this biostratigraphic framework, *Chiropteridium lobospinosum*, the most distinctive and widespread species among the 'mid'-Late Oligocene dinoflagellate markers, whose inception in the Mediterranean is in fact higher in the Rupelian (Biffi & Manum 1988; Wilpshaar et al. 1996; Torricelli 2000; Torricelli & Biffi 2001), was not found.

Calcareous nannofossil biostratigraphy of the Canale Candela section

Several integrated biostratigraphies including nannofossils have already been published on Upper Eocene-Oligocene sections in Italy (Roth et al. 1971, Proto Decima et al. 1975, Monechi 1986, Nocchi et al. 1986, Premoli Silva et al. 1988, Parisi et al. 1988). Berggren et al. (1995) gave an extensive review of the bibliography concerning the Paleogene calcareous nannofossil magnetobiochronology, whereas reference is made to Roth (1970), Perch-Nielsen (1985), Aubry (1986) and Backmann (1987) to find reviews on biostratigraphy and taxonomy.

Catanzariti et al. (1997) focused on the calcareous nannofossil biostratigraphy around the Eocene/Oligocene boundary within the terrigenous sediments of the Ranzano Formation (Epiligurian Succession) outcropping in the northern Apennines. As several remarks and suggestions of those authors well apply to the nannofossil record of the Canale Candela section, the work of Catanzariti et al. (1997) with corresponding biozonation (MNP zones) is herein considered as the main reference (Fig. 5).

Calcareous nannofossils are abundant and well-preserved throughout the lower part of the Canale Candela section (CAN -TTA 1 to 11) (Fig. 4a). By contrast, the upper part (CAN-TT 1 to 10) yielded less rich assemblages with poor preservation. Reworked specimens, mainly from the Upper Cretaceous, are scarce in the lower part of the section and increase in the upper part.

The nannofloral composition is homogeneous throughout the Canale Candela section. *Coccolithus pelagicus, Dictyococcites bisectus, Sphenolithus moriformis, Zygrablithus bijugatus* together with *Reticulofenestra* spp. and small placoliths make up the bulk of the association. Stratigraphically significant taxa are rare and their abundance patterns were assessed through additional counts.

Following Catanzariti et al. (1997), the First Common Occurrence (FCO) of *Ericsonia obruta*, indicating the base of SubZone MNP21b, can be recognized in sample CAN-TTA 2. In fact, above this sample the common and continuous occurrence of *E. obruta* is recorded. Due to the presence of only one sample below this level, the possibility that even the base of the section falls within SubZone MNP21b has to be considered.

Only sporadic occurrences of *Discoaster barbadiensis* and *Discoaster saipanensis* have been detected, thus suggesting the possibility that these specimens should be considered as reworked.

Although *E. subdisticha* has not been considered as a single species in the distribution chart, it must be noted that the abundance of *E. obruta* decreases in sample CAN-TTA 8. In comparing this evidence with palynological data (that identify the presence of the *Adi* Zone between samples CAN-TTA 7 and 9), it is possible to infer that this event approximates the *E. subdisticha* End of Acme originally proposed as the base of SubZone CP16b by Okada & Bukry (1970), and labeled as *E. obruta* End of Acme by Coccioni et al. (1988) in the Massignano section (central Italy).

The Last Occurrence (LO) of *Ericsonia formosa*, defining the top of SubZone MNP21b, has been ranked as a problematic event by Catanzariti et al. (1997), who define the LO of *E. formosa* at the end of its continuous occurrence with a frequency above 1-2%. In the present study, this datum is tentatively recognized in sample CAN-TT 2, although the frequency of *E. formosa* below that sample is sometimes lower. Nevertheless, the following elements, supporting the identification of Zones MNP21/MNP22, must be considered:

a) the FO of *Sphenolithus distentus* in sample CAN-TTA 10, that is reported as an additional event in the upper part of SubZone MNP21b by Catanzariti et al. (1997);

b) the occurrence of *Sphenolithus akropodus* among the transitional forms between *Sphenolithus predistentus* and *S. distentus*; the total range of this species is reported in the vicinity of the LO of *E. formosa* in the Iberia abyssal plain (de Kaenel & Villa 1996);

c) the relative increase of reworked Cretaceous specimens above sample CAN-TTA 11 (compare with Catanzariti et al. 1997, figs. 13, 23).

The uppermost samples of the Canale Candela section fall again within the lowermost part of Zone MNP22, since *E. obruta* is still commonly and continuously present, whereas younger bioevents, such as the inception of *Helicosphaera recta* (defining the base of the overlying Zone MNP23) and the inception of large specimens of *Cyclicargolithus abisectus* (>10μm), are not recorded. As documented also from the Ranzano Formation (Catanzariti et al. 1997), *Reticulofenestra umbilicus/hillae* and *Isthmolithus recurvus* occur discontinuously in the samples investigated. Hence, it is difficult to interpret the position of their LOs, that are likely higher than the top of the Canale Candela section.

Palynomorph biostratigraphy of the Tusa section

In the samples studied the organic matter is strongly affected by biological degradation and/or altered by thermal maturation. Therefore, the composition of the originally rich assemblages is certainly biased by these factors. Due to bad preservation, only part of

the palynological content is taxonomically identifiable. No high resolution palynostratigraphy is thus established for this section as previously done for the Canale Candela section. Nevertheless, it must be emphasized that all the taxa identified in samples from the Tusa section, including some Lower Oligocene markers, also occur in the Canale Candela section (Calabro/Lucano boundary), thus supporting a correlation between the volcaniclastic turbidite sequences in the two localities. The taxa found in both sections are highlighted with an asterisk in the taxonomic appendix.

Calcareous nannofossil biostratigraphy of the Tusa section

Samples from the lowermost part of the section (TUSB-1 to 8) have yielded poor nannofossil assemblages. From sample TUSB-9 upward, possibly due to more favourable lithologies, nannofossils become frequent and better preserved. However, the overall conditions of the assemblages, probably biased by preservational factors, forbid a quantitative approach to the nannofossil study. The analyses were thus restricted to a qualitative comparison with the nannofossil assemblages recovered from the Canale Candela section and results can be summarised as follows (Fig. 4b).

· *E. obruta* is present in most samples, being scarce to common in those yielding richer assemblages.

· *S. predistentus/distentus*, *S. distentus* and *S. akropodus* are recorded in the upper part of the section (from sample TUSB-9 upward).

· *R. daviesii* is common and its relative abundance increases toward the top of the section. This stratigraphic distribution is quite similar to that recorded in the Canale Candela section.

· Large *Reticulofenestra* spp. (10-12 μm) (see taxonomic appendix for further explanation) are present only from sample TUSB-9 upward. In the Canale Candela section these forms are recorded from sample CANTT-1 upward.

These data support a correlation of the Tusa section (particularly from sample TUSB-9 upward) with the upper part of the Canale Candela section (from sample CAN-TTA 11 upward). Late Cretaceous forms as those recorded from the upper part of the Canale Candela section and interpreted as reworked, are absent in the Tusa section.

Summary of bio-chronostratigraphic results and conclusions.

Samples from the Tusa Tuffite Formation cropping out at the Calabro-Lucano boundary (southern Italy) have yielded remarkably rich palynomorph and calcareous nannofossil assemblages. All key events defining the four dinoflagellate cyst zones established by Brinkhuis & Biffi (1993) in the lowermost Oligocene at the Massignano section (GSSP of the Eocene/Oligocene boundary) are recorded in the Canale Candela section in the same sequence of occurrence. Calcareous nannofossils provide perfectly consistent information, since a rejuvenation of typically lowermost Oligocene coccolith assemblages is documented in the section from bottom to top consistently with data published by Catanzariti et al. (1997) from a time equivalent turbidite suite in the northern Apennines. Hence, the integrated biostratigraphies herein discussed, correlated to bio- and magnetostratigraphically well calibrated sections from the northern Apennines (Catanzariti et al. 1997) and central Apennines (Brinkhuis & Biffi 1993; Coccioni et al. 1987), unequivocally indicate an earliest Oligocene age of the Tusa Tuffite Formation at the Canale Candela section. Accordingly, the Aquitanian-Burdigalian age proposed for the same section by Zuppetta et al. (1984) on the basis of poor foraminiferal data (only 3 samples retained as age-diagnostic out of 42 samples analysed) has to be rejected. The good exposure and the remarkable continuity of the series, together with the high resolution biostratigraphy obtained by means of dinoflagellate cyst and nannofossil events, suggest to retain the Canale Candela section as a regional reference for the Tusa Tuffite Formation.

Even though no similarly rich and well preserved palynomorph and nannofossil assemblages were obtained from the Tusa Tuffite Formation sampled at the the type-locality (Nebrodi Mountains, Sicily), their composition is definitely consistent with the bio-chronostratigraphic framework established for this unit at the Calabro/Lucano boundary.

These results allow to establish a broad correlation with other Lower Oligocene volcaniclastic-rich sequences of the northern Apennines and western Alps, and to review the significance of the Tusa Tuffite in the southern Apennines. More in detail, based on recently published data, the Tusa Tuffite is correlated to the Aveto-Petrignacola Sandstone of the Subliguride Domain (Elter et al. 1999), the Ranzano Sandstone of the Epiligurian succession (Cibin et al. 1998) and the Taveyanne Sandstone of Switzerland and Savoie (Latelin & Muller 1987). All these successions are in fact Early Oligocene in age. The Tusa Tuffite appears older than the others, being herein ascribed to earliest Oligocene (MNP21b-22 zones, 32.2 to 33.7 Ma on the timescale of Berggren et al. 1995). For the Ranzano Sandstone volcaniclastic intervals (Cibin et al. 1998), a late Early Oligocene age has been proposed (zones NP22-NP23, tie at 32.7 to 29.2 Ma on the timescale of Berggren et al. 1995). The Aveto-Petrignacola Sandstone has also been ascribed to the late Early Oligocene (MNP23 zone; see Elter et al. 1999), with a radiometric age dating at 29+-0.2 Ma (Mattioli 1997). Finally, the age of the Taveyanne Sandstone has been fixed with radiometric dating at about 32.5 Ma (Ruffini et al. 1995).

Apart from the slight regional diachronism, all data are consistent in placing the volcaniclastic events in a short time interval within the Early Oligocene. Other similarities strongly suggest a broad regional correlation. First, all the four successions are characterized by volcaniclastic layers interbedded with a background turbidite sedimentation where non-volcanic grains make up the bulk of the sediment. Deposition of such mixed sequences always occurs in physiographically complex basins, probably of small size, characterised by centripetal sediment flux from different sources. Volcaniclastic beds are rarely pure. More often, they are composed of mixed volcanic and non-volcanic grains. The nature of volcanic grains is generally andesitic, from a calc-alcaline synorogenic magmatism. Variations in the type of volcanic debris concern those parameters that are related to the mechanisms of transportation and emplacement (grain size of clasts, amount of volcanic ash, etc.).

All authors agree in stating that the volcanic debris is generally recycled but not reworked from older volcanic rocks. About the mechanism of emplacement of volcaniclastic beds, authors envisage different processes that are probably related to the location of the basins with respect to the volcanic centres. An epiclastic origin of the volcanic grains (subaerial erosion of primary volcanics) has been proposed for the Tusa Tuffite by Critelli et al. (1990). By contrast, Cibin et al. (1998) suggest a turbidity current reworking of primary submarine pyroclastics for the intercalations in the Ranzano Sandstone. Whatever the process, all agree that the volcanic grains must be considered nearly contemporaneous and thus place the volcanic events close in time to the redistribution of volcaniclastics in the basins via turbidity currents.

In conclusion, data collected in the field and summarised from other recent papers point to a single regional event of rise and erosion of a volcanic arc, occurring during a short time span in the Early Oligocene. The volcaniclastic sediment is redistributed in a number of small basins, probably not in direct communication but responding to similar dynamics. In this context, the Tusa Tuffite, as well as the Formations previously mentioned from the northern Apennines and the western Alps, have the significance of a bridge-unit between the subduction stage of the Alps/Apennines orogeny (Cretaceous-Late Eocene) and the collisional stage, recorded by the development of the first apenninic foredeep sequences (Late Oligocene Macigno and Numidian Flysch, in the northern and southern Apennines respectively).

Acknowledgements. G. Knezaurek, K. von Salis and J. B. Riding are acknowledged for providing comments and suggestions which improved the original version of the manuscript. Sample processing was carried out in ENI S.p.A. - Agip Division Laboratories by P. Casali, E. Zoppi and L. Bianchi. Thanks are given to G. Brandazzi (ENI S.p.A.) for his help in editing the photographic plates. This paper is published with the permission of ENI S.p.A.-Agip Division.

Taxonomic appendix

Dinoflagellate cysts, acritarchs and prasinophycean algae

Alphabetical listing of dinoflagellate cysts, acritarchs and prasinophycean algae recorded from the Canale Candela section (Calabro/Lucano boundary). Taxa which occur also in samples from the type-locality of the Tusa Formation (Sicily) are marked with *. The first number in parentheses refers to the position of the taxon in the quantitative distribution-chart (Fig. 3). Taxa illustrated are followed by plate and figure references. The generic allocation and authorship of dinoflagellate cyst species follow Williams et al. (1998).

Achilleodinium biformoides (Eisenack 1954) Eaton 1976 (1)
Achomosphaera alcicornu (Eisenack 1954) Davey & Williams 1966 (2; Plate 2, Fig. 8)
Achomosphaera sp. sensu Brinkhuis & Biffi 1993 (62; Plate 2, Fig. 7)
Areoligera semicirculata (Morgenroth 1966) Stover & Evitt 1978 (3; Plate 3, Fig. 10)
Areosphaeridium diktyoplokum (Klumpp 1953) Eaton 1971 (4; Plate 2, Fig. 9; Plate 3, Fig. 13)
**Ascostomocystis potane* Drugg & Loeblich Jr. 1967 (74)
**Charlesdowniea clathrata* (Eisenack 1938) Lentin & Vozzhennikova 1989 (5; Plate 2, Fig. 2)
Cordosphaeridium fibrospinosum Davey & Williams 1966 (6)
Cordosphaeridium gracilis (Eisenack 1954) Davey & Williams 1966 / *Cordosphaeridium inodes* (Klumpp 1953) Eisenack 1963 (7)
Cordosphaeridium minimum (Morgenroth 1966) Benedek 1972 (45)
**Cribroperidinium* spp. (50)
Dapsilidinium pseudocolligerum (Stover 1977) Bujak et al. 1980 (8)
**Deflandrea arcuata* Vozzhennikova 1967 (39; Plate 2, Fig. 19)
**Deflandrea granulata* Menéndez 1965 (40; Plate 3, Fig. 17)
**Deflandrea* cf. *heterophlycta* sensu Biffi and Manum, 1988 (30; Plate 3, Fig. 18)
Deflandrea leptodermata Cookson & Eisenack 1965 (51)
**Deflandrea phosphoritica* Eisenack 1938 (9; cf. Plate 2, Fig. 20)
Dinopterygium cladoides sensu Morgenroth 1966 (10)
Diphyes colligerum (Deflandre & Cookson 1955) Cookson 1965 (63)
Distatodinium tenerum (Benedek 1972) Eaton 1976 (46)
**Enneadocysta pectiniformis* (Gerlach 1961) Stover & Williams 1995 (11; Plate 2, Fig. 11; Plate 3, Fig. 11)
Gelatia inflata Bujak 1984 (60)
*Gen et sp. indet. of Biffi & Manum 1988 (75)
**Glaphyrocysta intricata* (Eaton 1971) Stover & Evitt 1978 (31)
**Glaphyrocysta semitecta* (Bujak et al. 1980) Lentin & Williams 1981 (41; Plate 3, Fig. 6)
Hemiplacophora semilunifera Cookson & Eisenack 1965 (49)
**Heteraulacacysta ?leptalea* Eaton 1976 (12; Plate 2, Fig. 6)
Homotryblium abbreviatum Eaton 1976 (64)
**Homotryblium aculeatum* Williams 1978 (14; Plate 3, Fig. 12)
**Homotryblium oceanicum* Eaton 1976 (65)
Homotryblium floripes ssp. *breviradiatum* (Cookson & Eisenack 1961) Lentin & Williams 1977 (55)
**Homotryblium plectilum* Drugg & Loeblich Jr. 1967 (13)
**Hystrichokolpoma rigaudiae* Deflandre & Cookson 1955 (32)
**Hystrichokolpoma salacia* Eaton 1976 (15; Plate 3, Fig. 5)
Impagidinium velorum Bujak 1984 (16; Plate 3, Fig. 7)
Impagidinium spp. (33)
**Lejeunecysta* spp. (17; Plate 3, Fig. 16)
**Lentinia serrata* Bujak 1980 (34; Plate 3, Figs. 14-15)
Lingulodinium pychnospinosum (Benedek 1972) Stover & Evitt 1978 (18)
**Nematosphaeropsis labyrinthus* (Ostenfeld 1903) Reid 1974 (42)
Nematosphaeropsis lemniscata Bujak 1984 (35, Plate 3, Fig. 9)
Odontochitina spp. (66)

Operculodinium centrocarpum (Deflandre & Cookson 1955) Wall 1967 (36)
Operculodinium cf. *hirsutum* sensu Gocht 1969 (43, Plate 2, Fig. 10)
Operculodinium microtriainum (Klumpp 1953) Islam 1983 (19)
**Palaeocystodinium golzowense* Alberti 1961 (37)
Pentadinium goniferum Edwards 1982 (56)
**Pentadinium laticinctum* Gerlach 1961 (20)
Phthanoperidinium comatum (Morgenroth 1966) Eisenack & Kjellström 1972 (53)
Phthanoperidinium multispinosum Bujak, in Bujak et al. 1980 (67; Plate 3, Fig. 4)
Phthanoperidinium powellii Bujak 1994 (57)
Polysphaeridium zoharyi (Rossignol 1962) Bujak et al. 1980 (21)
Reticulatosphaera actinocoronata (Benedek 1972) Bujak & Matsuoka 1986 (22)
**Rhombodinium draco* Gocht 1955 (23; Plate 2, Fig. 3)
Rottnestia borussica (Eisenack 1954) Cookson & Eisenack 1961 (24; Plate 3, Figs. 2-3)
Samlandia chlamydophora Eisenack 1954 (25; Plate 3, Fig. 1)
**Schizosporis* sp. of Brinkuis & Biffi 1993 (71; Plate 3, Fig. 12)
**Schizosporis* spp. (73; Plate 3, Fig. 13)
Selenopemphix nephroides Benedek 1972 (26)
Spiniferites mirabilis (Rossignol 1964) Sarjeant 1970 (47)
**Spiniferites pseudofurcatus* (Klumpp 1953) Sarjeant (27)
**Spiniferites gr. ramosus* (Ehrenberg 1938) Mantell 1954 (28)
Systematophora ancyrea Cookson & Eisenack 1965 (52)
Tenua hystrix Eisenack 1958 (61)
**Thalassiphora pelagica* (Eisenack 1954) Eisenack & Gocht 1960 (29)
Thalassiphora succincta Morgenroth 1966 (48; Plate 3, Fig. 8)
Thalassiphora? sp. sensu Brinkhuis & Biffi 1993 (38; Plate 2, Fig. 5)
Tuberculodinium vancampoae (Rossignol 1962) Wall 1967 (54)
Wetzeliella gochtii Costa & Downie 1976 (58; Plate 2, Fig. 4)
Wetzeliella symmetrica Weiler 1956 (59; Plate 2, Fig. 1)

Terrestrial sporomorphs

Alphabetical listing of terrestrially-derived sporomorphs recorded in the Canale Candela section (Calabro/Lucano boundary). Taxa which occur also in samples from the type-locality of the Tusa Formation (Sicily) are marked with *. The number in parentheses refers to the position in the quantitative distribution-chart (Fig. 3). The generic allocation and authorship of pollen and spore species follow Germeraad et al. (1968) and Legoux (1978).

*Bisaccate pollen
Cicatricosisporites dorogensis Potonié & Gelletich 1933 (69)
Classopollis spp. (80)
Echiperiporites estelae Germeraad, Hopping & Muller 1968 (79)
Leiotriletes spp. (76)
**Magnastriatites howardii* Germeraad, Hopping & Muller 1968 (78)
**Pediastrum* spp. (70)
**Retitricolporites* sp. (81)
Verrucatosporites usmensis (Van Der Hammen) Germeraad, Hopping & Muller 1968 (72)
Zlivisporis sp. (77)

Calcareous nannofossils

A full listing of taxa cited in text and figures is given below. Further references can be found in Perch-Nielsen (1985). The first number in parentheses refers to the position of the taxon in the quantitative distribution-chart of the Canale Candela section (Fig. 4a). The second number in parentheses, whenever present, refers to the position of the taxon in the distribution-chart of the Tusa section (Fig. 4b). Taxa illustrated are followed by plate and figure references.

Chiasmolithus oamaruensis (Deflandre, 1954) Hay, Mohler & Wade, 1966 (3, 27)
Cyclicargolithus abisectus (Muller, 1970) Wise, 1973
Cyclicargolithus floridanus (Roth & Hay in Hay et al., 1976) Bukry, 1971
Coccolithus eopelagicus (Bramlette & Riedel, 1954) Bramlette & Sullivan, 1961 (1, 23, Plate 4, Fig. 6)
Coccolithus pelagicus (Wallich, 1887) Schiller, 1930 (2, 1)
Cribrocentrum reticulatum (Gartner & Smith, 1967) Perch-Nielsen, 1971 (4)
Dictyococcites bisectus Hay, Mohler & Wade, 1966 (5, 2, Plate 4, Figs. 2, 3)
Discoaster barbadiensis Tan, 1927 (6, Plate 4, Fig. 8)
Discoaster deflandrei Bramlette & Riedel, 1954 (28, 14, Plate 4, Figs. 13, 14)
Discoaster saipanensis Bramlette & Riedel, 1954 (8, 13, Plate 4, Figs. 11, 12)
Discoaster tanii Bramlette & Riedel, 1954 (7, 3, Plate 4, Fig. 10)
Ericsonia formosa (Kampter, 1963) Haq, 1971 (9, 4, Plate 4, Fig. 1)
Ericsonia obruta Perch-Nielsen, 1971 (10, 5, Plate 4, Figs. 7, 8, 24)
Ericsonia subdisticha Roth & Hay in Hay et al., 1976
Ericsonia spp. (11)
Helicosphaera bramlettei Muller, 1970 (13, 17, Plate 4, Fig. 20)
Helicosphaera compacta Bramlette & Wilcoxon, 1967 (14, 15, Plate 4, Figs. 16, 17, 21)
Helicosphaera dinesenii Perch-Nielsen, 1971 / *Helicosphaera heezenii* Bukry, 1971 (26, 21)
Helicosphaera euphratis Haq, 1966 (25)
Helicosphaera lophota Bramlette & Sullivan, 1961 (33)
Helicosphaera recta Haq, 1966
Helicosphaera reticulata Bramlette & Wilcoxon, 1967 (27, 26, Plate 4, Figs. 18, 19)
Helicosphaera spp. (12)
Isthmolithus recurvus Deflandre, 1954 (15, 18, Plate 4, Fig. 4)
Lanternithus minutus Stradner, 1962 (16, 6, Plate 4, Fig. 22)
Reticulofenestra daviesii (Haq, 1968) Backmann, 1980 (17, 7, Plate 4, Fig. 23)
Reticulofenestra umbilicus (Levin, 1965) Martini & Ritzkowski, 1968 / *Reticulofenestra hillae* Bukry & Percival (18, 16, Plate 4, Fig. 5)
Reticulofenestra spp. (36, 22): here are grouped large reticulofenestrid (10-12 μm) morphologically related to *Dictyococcites bisectus* [e.g. *Reticulofenestra stavensis* (Levin & Joerger, 1967) Varol, 1989].
Rhabdosphaera pinguis Deflandre in Deflandre & Fert, 1954 (Plate 4, Fig. 15)
Rhabdosphaera spp. (31, 19)
Small Placoliths (19, 8): in this informal category *Cyclicargolithus floridanus* is grouped together with small and medium sized (up to 7-8 μm) reticulofenestrids. It is not in the scope of this work to go deeper into taxonomy of the *Reticulofenestra* species. For a comprehensive discussion of this topic, reference is made to De Kaenel & Villa (1996).
Sphenolithus akropodus De Kaenel & Villa, 1996 (35, 20, Plate 4, Figs. 28, 29)
Sphenolithus distentus (Martini, 1965) Bramlette & Wilcoxon, 1967 (29, 25, Plate 4, Fig. 30)
Sphenolithus moriformis (Bronnimann & Stradner, 1960) Bramlette & Wilcoxon, 1967 (20, 9)
Sphenolithus predistentus Bramlette & Wilcoxon, 1967 (21, 10, Plate 4, Figs. 25-27)
Sphenolithus radians Deflandre in Grassè, 1952 (30)
Toweius spp. (22)
Traversopontis spp. (34)
Zygrhablithus bijugatus (Deflandre in Deflandre & Fert, 1954) Deflandre, 1959 (23-24, 11-12)

REFERENCES

Aubry M.-P. (1986) - Paleogene calcareous nannoplankton biochronology of Northwestern Europe. *Palaeogeogr., Palaeoclim., Palaecol.*, 55: 267-334, Amsterdam.

Backmann J. (1987) - Quantitative calcareous nannofossil biochronology of middle Eocene through early Oligocene sediment from DSDP Sites 522 and 523. *Abh. Geol. B.* -A., 39: 21-31, Wien.

Berggren W.A., Kent D.V., Swisher II C.C. & Aubry M.-P. (1995) - A revised Cenozoic Geochronology and Chronostratigraphy. In: Berggren W.A., Kent D.V., Aubry M.-P. and Hardenbol J. (Eds.): Geochronology Time Scales and Global Stratigraphic Correlation. *SEPM Spec. Pub.* 54: 385 pp., Tulsa.

Biffi U. & Manum S.V. (1988) - Late Eocene-Early Miocene dinoflagellate cyst stratigraphy from the Marche Region (Central Italy). *Boll. Soc. Paleont. It.*, 27: 163-212, Modena.

Blow W.H. (1969) - Late Middle Eocene to Recent planktonic foraminiferal biostratigraphy. In: Brönniman R. and Renz N.H. (eds.), *Proceedings of the First International Conference on Planktonic Microfossils*, 1967: 199-421, Geneva.

Bouma A.H. (1962) - Sedimentology of some Flysch deposits, a graphic approach to facies interpretation. Elsevier Co., 168 pp., Amsterdam.

Brinkhuis H. (1994) - Late Eocene to Early Oligocene dinoflagellate cysts from the Priabonian type-area (Northeast Italy): biostratigraphy and paleoenvironmental interpretation. *Palaeogeogr., Palaeoclim., Palaecol.*, 107: 121-163, Amsterdam.

Brinkhuis H & Biffi U. (1993) - Dinoflagellate cyst stratigraphy of the Eocene/Oligocene transition in central Italy. *Mar. Microp.*, 22: 131-183, Amsterdam.

Catanzariti R., Rio D. & Martelli L. (1997) - Late Eocene to Oligocene calcareous nannofossil biostratigraphy in northern Apennines: the Ranzano sandstone. *Mem. Sci. Geol.*, 49: 207-253, Padova.

Cibin U., Tateo F., Catanzariti R., Martelli L. & Rio D. (1998) - Composizione, origine ed età del vulcanesimo andesitico oligocenico inferiore dell'Appennino settentrionale: le intercalazioni vulcano-derivate nella Formazione di Ranzano. *Boll. Soc. Geol. It.*, 117: 569-591, Roma.

Coccioni R., Monaco P., Monechi S., Nocchi M. & Parisi G. (1988) - Biostratigraphy of the Eocene-Oligocene boundary at Massignano (Ancona, Italy). In Premoli Silva I., Coccioni R. and Montanari A. (Eds.). The Eocene-Oligocene Boundary in the Umbria-Marche basin (Italy). Int. Subcomm. Paleog. Strat., E/O Meeting, Ancona 1987, Spec. Publ.: pp. 59-80, Ancona.

Critelli S., De Rosa R., Sonnino M. & Zuffa G.G. (1990) - Significato dei depositi vulcanoclastici della Formazione delle Tufiti di Tusa (Miocene inferiore, Lucania meridionale). *Boll. Soc. Geol. It.*, 109: 743-762, Roma.

De Capoa P., Guerrera F., Perrone V., Serrano F. & Tramontana M. (2000) - The onset of the syn-orogenic sedimentation in the Flysch Basin of the Sicilian Maghrebids: state of the art and new biostratigraphic constraints. *Ecl. Geol. Helv.*, 93: 65-79, Basel.

De Kaenel E. & Villa G. (1996) - Oligocene-Miocene calcareous nannofossil biostratigraphy and paleoecology from the Iberia abyssal plain. In Whitmarsh R.B. et al. (Eds.), *Proc. ODP, Sci. Res.*, 149: 79-145, College Station (TX).

Edwards D.A., Leeder M.R., Best J.L. & Pantin H.M. (1994) - On experimental reflected density currents and the interpretation of certain turbidites. *Sedimentology*, 41: 437-461, Amsterdam.

Elter P., Catanzariti R., Ghiselli F., Marroni M., Molli G., Ottria G. & Pandolfi L. (1999) - L'Unità Aveto (Appennino settentrionale): caratteristiche litostratigrafiche, biostratigrafia, petrografia delle areniti ed assetto strutturale. *Boll. Soc. Geol. It.*, 118: 41-63, Roma.

Fornaciari E., Di Stefano A., Rio D. & Negri A. (1996) - Middle Miocene quantitative calcareous nannofossil biostratigraphy in the Mediterranean Region. *Micropaleontology*, 42: 37-63, New York.

Fornaciari E. & Rio D. (1996) - Latest Oligocene to Early Miocene quantitative calcareous nannofossil biostratigraphy in the Mediterranean region. *Micropaleontology*, 42: 1-36, New York.

Germeraad J.H., Hopping C.A. & Muller J. (1968) - Palynology of Tertiary sediments from tropical areas. *Review of Palaeobotany & Palynology*, 6: 189-348, Amsterdam.

Gocht H. (1969) - Formengemeinschaften alttertiären microplanktons aus Bohrproben des Erdölfedes Meckelfels Bei Homburg. *Palaeontographica* Abt B, 126: 1-100, Stuttgart.

Guerrera F. & Wezel F.C. (1974) - Nuovi dati stratigrafici sui Flysch Oligo-Miocenici siciliani e considerazioni tettoniche relative. *Rivista Mineraria Siciliana*, 25 (145-147): 27-51, Palermo.

Latelin O. & Muller D. (1987) - Evolution paleogeographique du bassin des Gres de Taveyannaz dans les Arvais (haute Savoie) a la fin du Paleogene. *Ecl. Geol. Helv.*, 80: 127-140, Basel.

Legoux O. (1978) - Quelques espèces de pollen caractéristiques du Néogène du Nigeria - Some characteristic species of pollen from the Neogene of Nigeria. *Bull. Cent. Rech. Expl.-Prod. Elf-Aquitaine*, 2: 265-317, Pau.

Lentini F. (1979) - Le Unità Sicilidi della Val d'Agri (Appennino Lucano). *Geol. Rom.*, 18: 215-224, Roma.

Maiorano P. (1998) - Miocene quantitative calcareous nannofossil biostratigraphy from southern Apennines foredeep deposits and Mediterranean DSDP site 372. *Riv. It. Paleont. Strat.*, 104: 391-416, Milano.

Martini E. (1971) - Standard Tertiary and Quaternary calcareous nannoplankton zonation. In: A. Farinacci (ed.), *Proceedings of the Second Conference on Planktonic Microfossils*, Rome 1970: 739-785, Roma.

Mattioli M. (1997) - Vulcanismo terziario nell'Appennino Settentrionale: evidenze da clasti andesitici nell'unità di Canetolo e da corpi vulcanici sepolti. *Acta Natur. Ateneo Parmense*, 33: 89-91, Parma.

Monechi S. (1986) - Calcareous nannofossil events around the Eocene/Oligocene boundary in the Umbrian Apennines (Italy). *Palaeogeogr., Palaeoclim., Palaeoecol.*, 57: 61-69, Amsterdam.

Morgenroth P. (1966) - Mikrofossilen und Konkretionen des

Nordwesteuropäischen Untereozäns. *Palaeontographica* Abt B, 119: 1-53, Stuttgart.

Mutti E. (1992) - Turbidite Sandstones. *Special Publication AGIP S.p.A.-Università di Parma*, 275 pp., San Donato Milanese.

Mutti E. & Normark W.R. (1987) - Comparing examples of modern and ancient turbidite systems: problems and concepts. In: J.K. Leggett and G.G. Zuffa (Eds.), *Marine Clastic Sedimentology: Concepts and Case Studies*, Graham and Trotman: 1-38, London.

Nocchi M., Parisi G., Monaco P., Monechi S., Madile M., Napoleone G., Ripepe M., Orlando M., Premoli Silva I. & Bice D.M. (1986) - The Eocene-Oligocene boundary in the umbriam pelagic sequences, Italy. In Ch. Pomerol and I. Premoli Silva (Eds.). Terminal Eocene Events.

Ogniben L. (1960) - Note illustrative dello schema geologico della Sicilia nord-orientale. *Riv. Mine. Sicil.*, 64-65: 183-212, Palermo.

Ogniben L. (1969) - Schema introduttivo alla geologia del confine calabro-lucano. *Mem. Soc. Geol. It.*, 8: 453-763, Roma.

Okada H. & Bukry D. (1980) - Supplementary modification and introduction of code numbers to the low latitude coccolith biostratigraphy zonation. *Mar. Micropal.*, 5: 321-324, Amsterdam.

Perch-Nielsen K. (1985) - Cenozoic calcareous nannofossils. In: Bolli H.M., Saunders J.B. and Perch-Nielsen K. (Eds.). *Plankton Stratigraphy*, pp. 427-554, Cambridge.

Pickering K.T. & Hiscott R.N. (1985) - Contained (reflected) turbidity currents from the Middle Ordovician Cloridorme Formation, Quebec, Canada: an alternative to the antidune hypotesis. *Sedimentology*, 32: 373-394, Amsterdam.

Premoli Silva I., Orlando M., Monechi S., Madile M. Napoleone G. & Ripepe M. (1988) - Calcareous Plankton Biostratigraphy and Magnetostratigraphy at the Eocene-Oligocene transition in the Gubbio Area. In Premoli Silva I., Coccioni R. and Montanari A. (Eds.). The Eocene-Oligocene Boundary in the Umbria-Marche basin (Italy). *Int. Subcomm. Paleog. Strat., E/O Meeting, Ancona 1987, Spec. Publ.*: pp. 137-161, Ancona.

Proto Decima F., Roth P.H. & Todesco L. (1975) - Nannoplankton calcareo del Paleocene e dell'Eocene della sezione di Possagno. *Schweiz. Palaont. Abhandl.*, 97: 35-161, Basel.

Romein A.J.T. (1979) - Lineages in Early Paleogene calcareous nannoplankton. *Utrecht Micropaleont. Bull.*, 22: 231 pp., Utrecht.

Roth P.H. (1970) - Oligocene Calcareous Nannoplankton Biostratigraphy. *Ecl. Geol. Helv.*, 63: 799-881, Basel.

Roth P.H., Baumann P. & Bertolino V. (1971) - Late Eocene-Oligocene calcareous nannoplankton from central and northern Italy. In: A. Farinacci (ed.), *Proceedings of the Second Conference on Planktonic Microfossils, Rome* 1970: 739-785, Roma.

Ruffini R., Cosca M.A., D'Atri A., Hunziker J.C. & Polino R. (1995) - The volcanic supply of the Taveyanne turbidites (Savoie, France): a riddle for alpine volcanism. In: R. Polino and R. Sacchi (eds.), *Rapporti Alpi-Appennino, atti del convegno, Peveragno* 31/5-1/6 1994, Acc. Naz. Lincei Scritti e Documenti, 15: 359-376, Roma.

Torricelli S. (2000) - Palynology of the Numidian Flysch of northern Tunisia: a key to a revised stratigraphic model. *Proceedings of the 7th Tunisian Petroleum Exploration & Production Conference, Tunis*, April 3-7, 2000.

Torricelli S. & Biffi U. (2001) - Palynostratigraphy of the Numidian Flysch of northern Tunisia (Oligocene-Early Miocene). *Palynology* 25: 29-55, Dallas.

Wezel F.C. (1973) - Nuovi dati sull'evoluzione e posizione strutturale del Flysch di Tusa in Sicilia. *Boll. Soc. Geol. It.*, 92: 193-211, Roma.

Williams G. L., Lentin J.K. & Fensome R.A. (1998) - The Lentin and Williams Index of Fossil Dinoflagellates 1998 Edition. *Am. Assoc. Stratigr. Palynol. Contrib. Ser.*, 34: 817 pp., Dallas.

Wilpshaar M., Santarelli A., Brinkhuis H. & Visscher H. (1996) - Dinoflagellate cysts and mid-Oligocene chronostratigraphy in the central Mediterranean region. *Journ. Geol. Soc.*, 153: 553-561, London.

Zuppetta A., Russo M. & Turco E. (1984) - Alcune osservazioni sulle 'Tufiti di Tusa' nell'area compresa tra la Valsinni e Rocca Imperiale (confine calabro-lucano). *Boll. Soc. Geol. It.*, 103: 623-627, Roma.